European Journal of Medicinal Chemistry 300 (2025) 118095

Contents lists available at ScienceDirect

European Journal of Medicinal Chemistry

journal homepage: www.elsevier.com/locate/ejmech

Research paper

From pan-active to parasite-selective antiparasitic agents: A scaffold hopping approach

Chiara Borsari [a,*], Nuno Santarem [b,c], Dina Coertzen [d], Asia Mazzolari [a], Alexandra Ioana Corfu [a], Catarina Coelho [e], Francisca Barbosa [e], Lucia Tamborini [a], Lyn-Marié Birkholtz [d,f], Lorenzo Raffellini [g], Oliver Keminer [h], Nicoletta Basilico [i], Silvia Parapini [j], Sheraz Gul [h], Anabela Cordeiro-da-Silva [b,c], Paola Conti [a]

[a] Department of Pharmaceutical Sciences, University of Milan, Via Mangiagalli 25, 20133, Milan, Italy
[b] Institute for Research and Innovation in Health (i3S), University of Porto, 4200-135, Porto, Portugal
[c] Department of Biological Sciences, Faculty of Pharmacy, University of Porto, 4050-313, Porto, Portugal
[d] Department of Biochemistry, Genetics and Microbiology, Institute for Sustainable Malaria Control, University of Pretoria, Hatfield, 0028, South Africa
[e] Host-Parasite Interaction Group, Institute for Research and Innovation in Health, University of Porto, 4200-135, Porto, Portugal
[f] Department of Biochemistry, Stellenbosch University, Matieland, Stellenbosch, 7602, South Africa
[g] Department of Pharmacy, University of Pisa, Via Bonanno 6, Pisa, 56126, Italy
[h] Fraunhofer Institute for Translational Medicine and Pharmacology ITMP, Discovery Research ScreeningPort, Schnackenburgallee 114, Hamburg, 22525, Germany
[i] Department of Biomedical, Surgical and Dental Sciences, University of Milan, Via Pascal 36, 20133, Milan, Italy
[j] Department of Biomedical Sciences for Health, University of Milan, Via Pascal 36, Milan, 20133, Italy

ARTICLE INFO

Keywords:
Human African trypanosomiasis
Leishmaniasis
Malaria
Scaffold hopping
1,2,4-Oxadiazole
Oxazole

ABSTRACT

Vector-borne parasitic diseases (VBPDs) represent a major global public health concern, with human African trypanosomiasis (HAT), Chagas disease, leishmaniasis, and malaria collectively threatening millions of people, particularly in developing regions. Climate change may further influence their transmission and geographic spread, increasing the global burden. As drug resistance continues to rise, there is an urgent need for novel therapeutic agents to expand treatment options and limit disease progression. Exploiting a cell-based phenotypic approach, we had previously developed 1,3,4-oxadiazole derivatives, as broad-spectrum low-toxicity agents active against protozoan parasites including *Plasmodium falciparum*, *Leishmania* spp. and *Trypanosoma brucei*. Herein, we applied a scaffold-hopping approach to develop novel chemotypes by replacing the central 1,3,4-oxadiazole core with 1,2,4-oxadiazole and oxazole rings. A systematic investigation allowed us to generate two novel libraries of compounds and carry out extensive Structure-Activity-Relationship studies and early drug discovery pharmacological liability characterization. Starting from pan-active 1,3,4-oxadiazole-based antiparasitic agents, we identified two anti-kinetoplastid molecules bearing the 1,2,4-oxadiazole core and one promising anti-*T. brucei* agent featuring an oxazole core. Our work paves the way for the development of novel chemotypes to successfully fight parasitic infections.

1. Introduction

Malaria and kinetoplastid diseases - Leishmaniasis, human African typanosomiasis and Chagas diseases - are vector-borne parasitic diseases (VBPDs) caused by parasites transmitted by vectors and represent significant health concerns [1,2]. Human African trypanosomiasis (HAT), fatal disease if untreated, is caused by infection with two subspecies of the protozoan parasite *Trypanosoma brucei* (*T. b. gambiense* and *T. b. rhodesiense*) [3,4]. These parasites are transmitted by tsetse flies of the genus *Glossina*. Chagas disease, also known as American trypanosomiasis, is a tropical parasitic disease caused by *Trypanosoma cruzi* and transmitted primarily by triatomine bugs (also known as "kissing bugs"). Leishmaniasis, caused by various *Leishmania* species and transmitted by sandflies, manifests in three main forms: visceral (VL), cutaneous (CL), and mucocutaneous, with an estimated 700,000 to 1 million new cases annually [5]. *Trypanosoma* and *Leishmania* species belong to a group of

* Corresponding author. Dept. of Pharmaceutical Sciences, University of Milan; Via Mangiagalli 25, Milan, 20133, Italy.
E-mail address: chiara.borsari@unimi.it (C. Borsari).

https://doi.org/10.1016/j.ejmech.2025.118095
Received 1 July 2025; Received in revised form 20 August 2025; Accepted 23 August 2025
Available online 29 August 2025

flagellated protozoans named kinetoplastids, which are characterized by the presence of a DNA-containing region, known as a kinetoplast, in their single large mitochondrion [6]. Malaria is caused by five species of *Plasmodium (P. falciparum, P. vivax, P. malariae*, *P. ovale* and *P. knowlesi*) transmitted through the bites of infected female *Anopheles* mosquitoes. *P. falciparum* accounts for over 90 % of global malaria-related deaths [7].

The spread of vector-borne diseases is influenced by a complex interplay of demographic, environmental and social factors. Although the burden of these diseases is prevalent in tropical and subtropical areas, global travel and trade, climate change as well as adaptation of the vectors contribute to the spread of VBPDs, poses considerable public health problems globally [8]. Some progress has been made by the global community in addressing these diseases through vector control, preventive interventions, and therapeutics. However, the available treatments are still associated with several drawbacks including toxicity, poor efficacy, and the emergence of resistance [9]. This highlights the need to discover new classes of antiparasitic agents with possible novel mechanisms of action [10]. Nonprofit organizations, such as the Bill and Melinda Gates Foundation, Drugs for Neglected Diseases (DNDi) and Medicines for Malaria Venture (MMV), academic institutions and industry have made significant steps toward VBPD's drug discovery [11]. The most recent and notable achievements are the development of fexinidazole for HAT [12] and the approval of tafenoquine, for preventing *P. vivax* malaria [13]. However, the discovery of new drugs active against protozoan parasites faces challenges due to the complex biology of these organisms, which can involve the need to target various intracellular development stages or affect the central nervous system (CNS).

Cell-based phenotypic screening is a powerful approach allowing for the identification of compounds that are active against the entire parasite. This method enables the evaluation of a compound interacting with one or more molecular targets, whilst meeting membrane permeability, solubility and intracellular stability requirements [14–18]. Moreover, this biology-first strategy may provide tool molecules to link a therapeutic effect to previously unknown signalling pathways [19]. Successful example of antiparasitic drug development for HAT using phenotypic screening approaches are fexinidazole, which was approved for treatment of HAT in 2018, and acoziborole (SCYX-7158), an orally-active benzoxaborole, for the treatment of stage 2 HAT that has shown promise in several clinical trials and is ongoing further clinical studies [20]. In addition, cipargamin, also discovered through a phenotypic approach, is currently undergoing phase II clinical trial for the treatment of *P. falciparum* malaria (NCT03334747) [21].

Using a cell-based phenotypic approach, we previously developed 1,3,4-oxadiazole derivatives, as broad-spectrum low-toxicity agents active against protozoan parasites including *P. falciparum*, *Leishmania* spp. and *T. brucei* [22]. To further optimize these small molecules, we decided to apply a scaffold hopping approach, a special type of bioisosteric replacement consisting in the substitution of the small molecule core structure [23]. For example, scaffold hopping involves modifying carbon and heteroatoms in the backbone ring of the core heterocycle of a bioactive molecule, while keeping connected functional groups and pharmacophores almost unaltered. In general, this strategy identifies a new chemotype with key ligand–target binding interactions conserved, while improving the physicochemical properties and the overall biological profile. In detail, our previously identified compounds are characterized by a central portion A (Fig. 1A) containing a 1,3,4-oxadiazole ring, linked to a 3-bromo-4,5-dihydroisoxazole (BDHI) moiety (portion B) and to a lipophilic tail (portion C). In the present work, we decided to keep portion B constant, since the BDHI moiety is reported to be a moderately reactive and drug-like warhead, capable of irreversibly inactivating target proteins by reacting with nucleophilic residues, especially with activated cysteine residues, and we applied our scaffold hopping approach to the central portion A [24,25]. In portion C, we inserted the same set of substituents previously investigated [22], in order to easily dissect the role of the core-heterocycle modification. Therefore, we designed two novel compound libraries, namely series I, containing a 1,2,4-oxadiazole as portion A, and series II, containing an oxazole ring (Fig. 1B). The libraries were characterized for their overall biological profile towards *T. brucei*, *Leishmania* spp. and *P. falciparum*, and their early drug discovery pharmacological liability properties were determined.

2. Chemistry

The series of novel 1,2,4-oxadiazole derivatives (**2a-2l**) was synthesized as depicted in Scheme 1. The Williamson ether synthesis was used to convert the commercially available 4-hydroxybenzaldehyde **4** into the corresponding ethers **5a-5e** and **5g-5l** by treatment with the desired alkyl bromides in the presence of solid K_2CO_3 as a base in refluxing acetone. This reaction generally proceeded with good yield, with a few exceptions. The poor reaction yield observed for the cyclopentanemethyl derivative **5f** required the development of a different synthetic procedure. A Mitsunobu reaction between **4** and cyclopentanemethanol, in the presence of DIAD and PPh_3, was performed to obtain the desired intermediate **5f** in a 57 % yield. A one pot procedure involving the conversion of the aldehyde group into an aldoxime, followed by its acetylation, and loss of acetic acid was carried out by refluxing hydroxylamine hydrochloride and acetic anhydride in pyridine to obtain nitriles **6a-6l**. The nucleophilic attack of hydroxylamine on nitriles was performed following Tiemann's method [26] treating the nitrile-substituted intermediates **6a-6l** with hydroxylamine hydrochloride and Na_2CO_3 in a refluxing ethanol/water mixture to give amidoximes **7a-7l**. Chemo-selective *O*-acylation of amidoximes **7a-7l** was achieved using acryloyl chloride in dry THF affording the

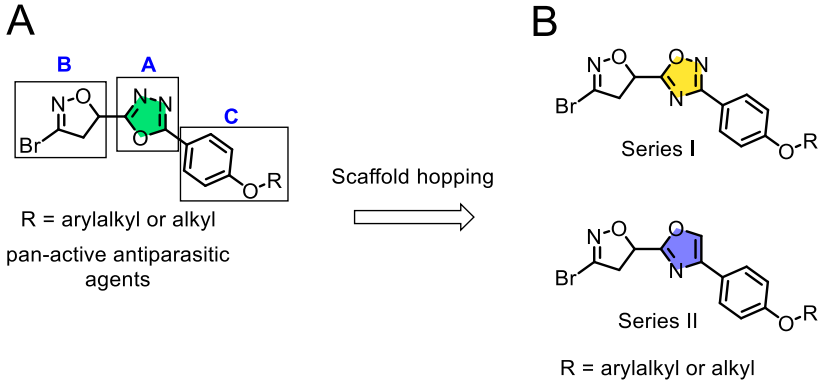

Fig. 1. A) Previously investigated 1,3,4-oxadiazole derivatives as pan-active antiparasitic agents. **B)** Scaffold hopping approach for the development of novel 1,2,4-oxadiazole (series I) and oxazole ring (series II) chemotypes.

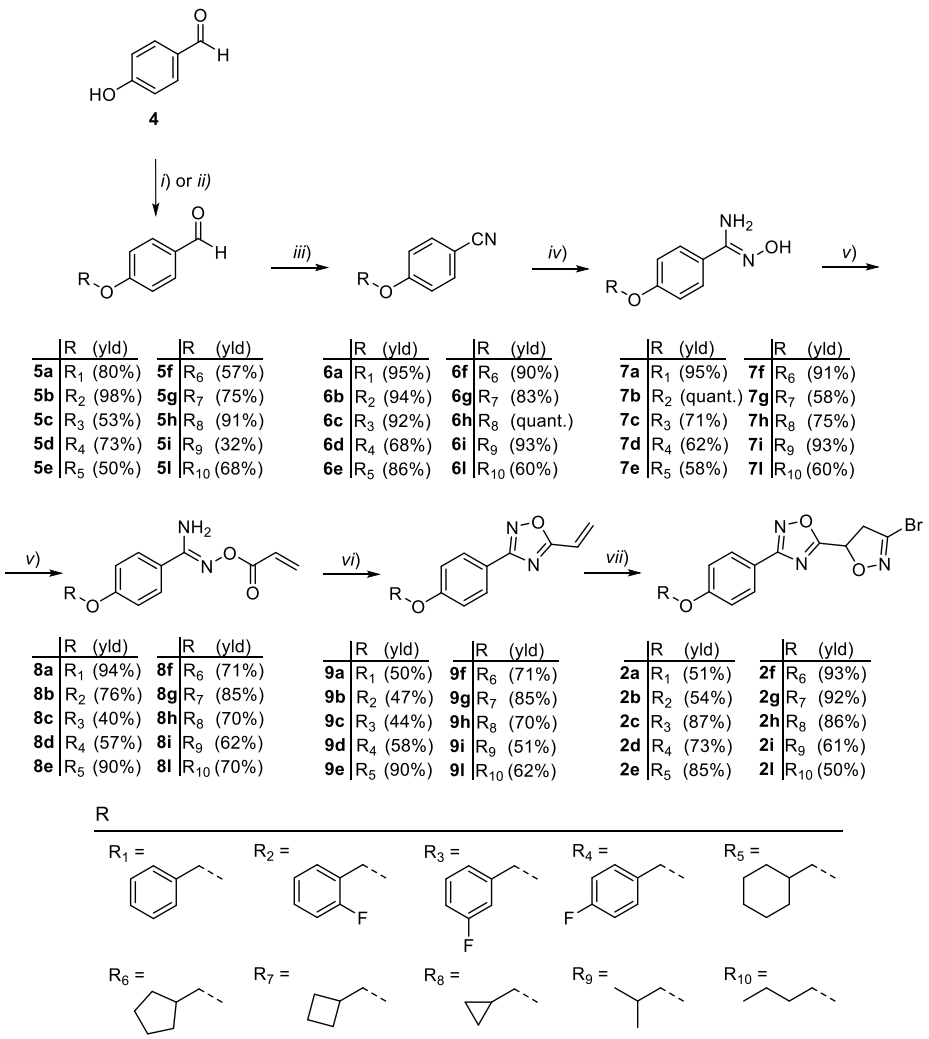

	R (yld)		R (yld)
5a	R_1 (80%)	**5f**	R_6 (57%)
5b	R_2 (98%)	**5g**	R_7 (75%)
5c	R_3 (53%)	**5h**	R_8 (91%)
5d	R_4 (73%)	**5i**	R_9 (32%)
5e	R_5 (50%)	**5l**	R_{10} (68%)

	R (yld)		R (yld)
6a	R_1 (95%)	**6f**	R_6 (90%)
6b	R_2 (94%)	**6g**	R_7 (83%)
6c	R_3 (92%)	**6h**	R_8 (quant.)
6d	R_4 (68%)	**6i**	R_9 (93%)
6e	R_5 (86%)	**6l**	R_{10} (60%)

	R (yld)		R (yld)
7a	R_1 (95%)	**7f**	R_6 (91%)
7b	R_2 (quant.)	**7g**	R_7 (58%)
7c	R_3 (71%)	**7h**	R_8 (75%)
7d	R_4 (62%)	**7i**	R_9 (93%)
7e	R_5 (58%)	**7l**	R_{10} (60%)

	R (yld)		R (yld)
8a	R_1 (94%)	**8f**	R_6 (71%)
8b	R_2 (76%)	**8g**	R_7 (85%)
8c	R_3 (40%)	**8h**	R_8 (70%)
8d	R_4 (57%)	**8i**	R_9 (62%)
8e	R_5 (90%)	**8l**	R_{10} (70%)

	R (yld)		R (yld)
9a	R_1 (50%)	**9f**	R_6 (71%)
9b	R_2 (47%)	**9g**	R_7 (85%)
9c	R_3 (44%)	**9h**	R_8 (70%)
9d	R_4 (58%)	**9i**	R_9 (51%)
9e	R_5 (90%)	**9l**	R_{10} (62%)

	R (yld)		R (yld)
2a	R_1 (51%)	**2f**	R_6 (93%)
2b	R_2 (54%)	**2g**	R_7 (92%)
2c	R_3 (87%)	**2h**	R_8 (86%)
2d	R_4 (73%)	**2i**	R_9 (61%)
2e	R_5 (85%)	**2l**	R_{10} (50%)

Scheme 1. Synthesis of compounds **2a-2l**. Reagents and conditions: i) R–Br, K_2CO_3, acetone, reflux, o/n (for **5a-5e**, **5g-5l**); ii) PPh_3, DIAD, cyclopentanemethanol, dry THF, o/n (for **5f**); iii) $NH_2OH{\cdot}HCl$, pyridine, Ac_2O, reflux, 2–3 h; iv) $NH_2OH{\cdot}HCl$, Na_2CO_3, EtOH/H_2O, 85 °C, o/n; v) acryloyl chloride, dry THF, 0 °C → rt, 1–2 h; vi) TBAF 1 M in dry THF, rt, 1–2 h; vii) DBF, $NaHCO_3$, EtOAc, rt, o/n. The final compounds were tested as racemic mixtures.

O-acrylamidoximes **8a-8l**. The following cyclization reaction was performed with a catalytic amount of TBAF in dry THF at room temperature, to obtain the oxadiazole derivatives **9a-9l** [27]. Intermediates **9a-9l** present a vinyl substituent in position 5, which is a good dipolarophile exploited for the following 1,3-dipolar cycloaddition to form the BDHI core. Thus, intermediates **9a-9l** reacted with bromonitrile oxide, generated *in situ* from its stable precursor dibromoformaldoxime (DBF) [28] in an AcOEt/$NaHCO_3$ heterogeneous mixture, to obtain final compounds **2a-2l** with good to excellent yield (50–93 %).

The oxazole-bearing compounds **3a-3l** were prepared following a multi-step synthesis (Scheme 2). The ethers-substituted ketones **11a-11l** were synthesized following the Williamson ether synthesis previously described and obtained with good to excellent yield (>63 %, quantitative). The Mitsunobu reaction between 4-hydroxyacetophenone **10** and cyclopentanemethanol gave compound **11f** with 75 % yield. The resulting intermediates **11a-11b** and **11l** were converted into their respective α-bromo-ketones **12a-12b** and **12l** using copper(II) bromide as bromination agent in refluxing ethyl acetate overnight. Due to the formation of several by-products leading to purification difficulties, the α-bromination of ketones **11c-11i** was carried out in chloroform by adding Br_2. The reaction time was significantly reduced with respect to the $CuBr_2$ procedure (30–60 min *vs* overnight) and the dibrominated by-product was not observed, making the purification process easier. Afterwards, a Delépine reaction was used to convert α-bromo-ketones **12a-12l** into the corresponding amines, obtained as hydrochloride salts (**13a-13l**). The reaction proceeded by treating the alkylbromides with hexamethylenetetramine followed by hydrolysis of the quaternary ammonium salt in a refluxing solution of concentrated hydrochloric acid and methanol. Acylation of amines **13a-13l** was achieved using acryloyl chloride in dry dichloromethane and Na_2CO_3 as base to give the *N*-acylated intermediates **14a-14l**. A subsequent cyclization reaction with phosphorus oxychloride gave the corresponding 5-substituted-2-vinyl-oxazole derivatives (**15a-15l**). The vinyl-substituted derivatives (**15a-15l**) were submitted to 1,3-dipolar cycloaddition with bromonitrile oxide generated *in situ* from DBF [28], as described for the 1,2,4-oxadiazole derivatives. The reaction mixture was vigorously stirred overnight at room temperature to obtain the desired final products **3a-3l** (Scheme 2).

3. Results and discussion

3.1. SAR study and anti-T. brucei agent selection

The novel series of 1,2,4-oxadiazole and oxazole derivatives was screened, as racemic mixtures, towards the bloodstream form of *T. brucei brucei*, and the data were compared with those obtained with the 1,3,4-oxadiazole-bearing compounds. Moreover, cytotoxicity was assessed using THP-1 macrophage-like cells, and the half maximal cytotoxicity

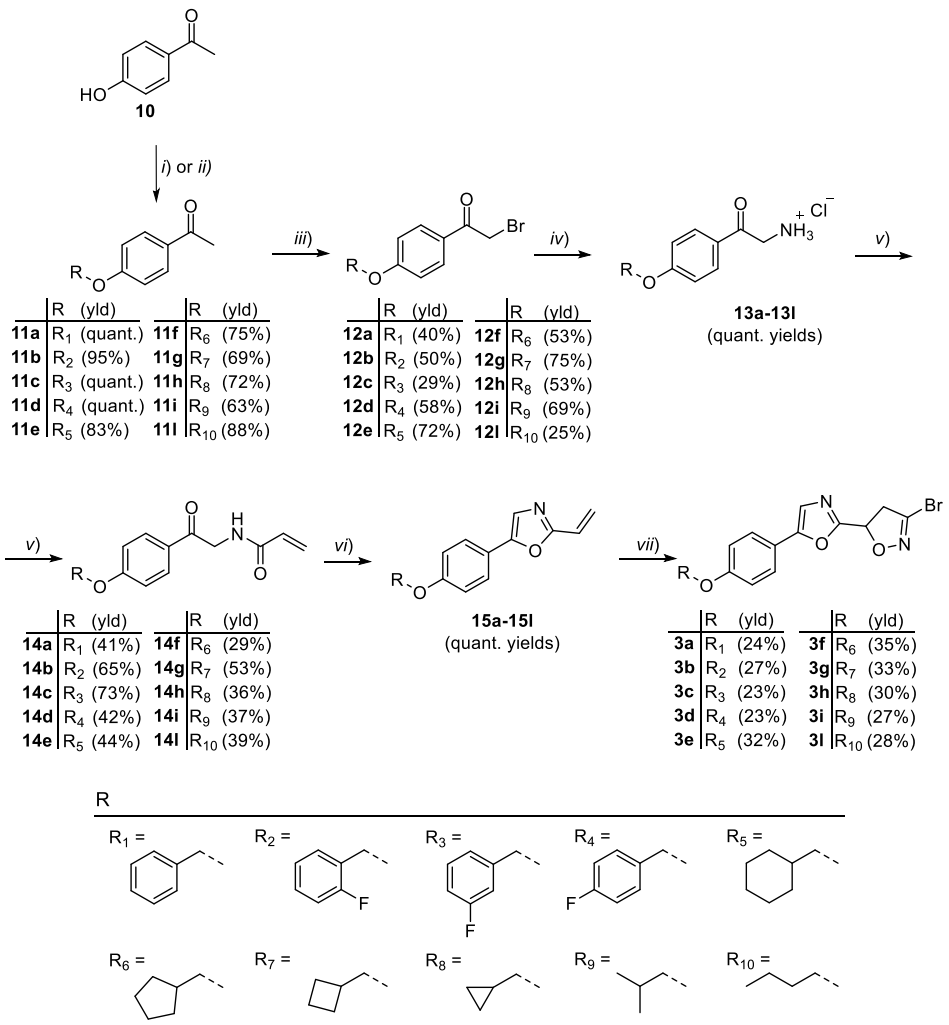

	R	(yld)		R	(yld)
11a	R_1	(quant.)	**11f**	R_6	(75%)
11b	R_2	(95%)	**11g**	R_7	(69%)
11c	R_3	(quant.)	**11h**	R_8	(72%)
11d	R_4	(quant.)	**11i**	R_9	(63%)
11e	R_5	(83%)	**11l**	R_{10}	(88%)

	R	(yld)		R	(yld)
12a	R_1	(40%)	**12f**	R_6	(53%)
12b	R_2	(50%)	**12g**	R_7	(75%)
12c	R_3	(29%)	**12h**	R_8	(53%)
12d	R_4	(58%)	**12i**	R_9	(69%)
12e	R_5	(72%)	**12l**	R_{10}	(25%)

	R	(yld)		R	(yld)
14a	R_1	(41%)	**14f**	R_6	(29%)
14b	R_2	(65%)	**14g**	R_7	(53%)
14c	R_3	(73%)	**14h**	R_8	(36%)
14d	R_4	(42%)	**14i**	R_9	(37%)
14e	R_5	(44%)	**14l**	R_{10}	(39%)

	R	(yld)		R	(yld)
3a	R_1	(24%)	**3f**	R_6	(35%)
3b	R_2	(27%)	**3g**	R_7	(33%)
3c	R_3	(23%)	**3h**	R_8	(30%)
3d	R_4	(23%)	**3i**	R_9	(27%)
3e	R_5	(32%)	**3l**	R_{10}	(28%)

Scheme 2. Synthesis of compounds **3a-3l**. Reagents and conditions: i) R–Br, K_2CO_3, acetone, reflux, o/n (for **11a-11e, 11g-11l**); ii) PPh_3, DIAD, cyclopentanemethanol, dry THF, o/n (for **11f**); iii) $CuBr_2$, dry EtOAc, reflux, o/n (for **12a**, **12b** and **12l**); Br_2, chloroform, 0 °C → rt (for **12c-12i**); iv) hexamine, DCE, 60 °C, 1 h; 12 M HCl, MeOH, 65 °C, 1 h v) acryloyl chloride, Na_2CO_3, dry DCM, rt, 1 h; vi) $POCl_3$, reflux, 2 h; vii) DBF, $NaHCO_3$, EtOAc, rt, o/n. The final compounds were tested as racemic mixtures.

concentration (CC_{50}) and the Selectivity Index (SI═CC_{50}/IC_{50} parasite) were calculated for the entire set of compounds. The general trend was that the 1,2,4-oxadiazole isomers showed a higher anti-*T. brucei* potency compared to their corresponding 1,3,4 regioisomers. In particular, the 1,2,4 regioisomers bearing a benzyl (**2a**) or an *ortho*-fluorobenzyl group (**2b**) were 4 to 6-fold more potent than the 1,3,4-oxadiazoles derivatives **1a** and **1b**, and associated with good SI (Table 1). The shift of the fluorine from *ortho* to *meta* (**2c**) and *para* (**2d**) positions resulted in a slight decrease in anti-*T. brucei* activity. The oxazole derivatives exhibited a 3.5-fold reduced activity compared to their 1,2,4-oxadiazole counterparts and showed similar or slightly lower activity compared to the 1,3,4-oxadiazole analogues, with the notable exception of compound **3h** (Table 1). All novel benzyl-substituted derivatives (**2a-2d** and **3a-3d**) displayed a calculated LogP (cLogP) > 3.9 and CNS MPO scores <5, posing a challenge in the potential application in stage 2 HAT treatment. The CNS MPO score defines the desirability space for a drug aimed at targeting the CNS, and is calculated considering six physicochemical properties: molecular weight (MW), calculated partition coefficient (clogP), calculated distribution coefficient at pH 7.4 (clogD), topological polar surface area (TPSA), number of hydrogen-bond donors (HBDs) and most basic center (pK_a) [29]. Only molecules with *CNS MPO >5* are expected to cross the BBB. All cycloalkyl- and alkyl-substituted compounds bearing the 1,2,4-oxadiazole core (**2e-2l**) yielded significant activity towards *T. brucei*, with IC_{50} values < 2 μM. Among the 1,2,4-oxadiazoles, the molecules bearing a cyclopentyl, cyclobutyl and cyclopropyl ring (**2f-2h**) or a linear alkane chain (**2l**) presented a negligible cytotoxicity on THP-1 macrophage-like cells, resulting in SI > 25. However, their high lipophilicity (cLogP >3.8) led to CNS MPO scores <5 and decreases the likelihood of CNS penetration. The cyclopropyl-substituted oxazole **3h** was identified as the best performing anti-*T. brucei* agent since it combines excellent potency and SI (IC_{50} = 0.87 μM; SI > 57) with desirable physicochemical properties for BBB penetration (*CNS MPO = 5.51*), and favorable cLogP values > 3.9 (Fig. S1). In addition, compound **3h** outperformed its corresponding 1,3,4-oxadiazole, **1h**, derivative previously identified (Fig. S1) [22].

3.2. Investigation of anti-leishmanial potency

Given the promising anti-trypanosomal potential of our novel molecules, we investigated their activity on *Leishmania*, a related

Table 1
Comparison of anti-*T. brucei* activity of 1,3,4-, 1,2,4- oxadiazoles and oxazoles.

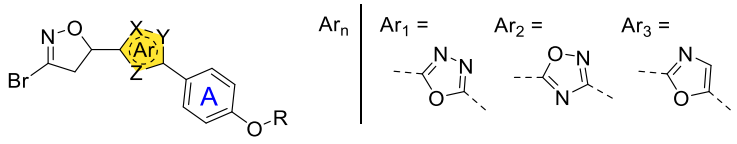

Comp.	Ar$_n$	R	IC$_{50}$ *T. brucei* (μM) and (range)	CC$_{50}$ (μM) and (range)	SI	clogP[a]	TPSA[a] (Å^2)	CNS MPO[a]
1a [22]	Ar$_1$	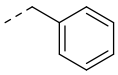	7.24 (5.91–8.70)	>100	>14	3.37	69.74	4.84
2a	Ar$_2$		1.79 (1.39–2.30)	100>CC$_{50}$ > 25	>14	4.78	69.74	3.82
3a	Ar$_3$		10.14 (9.02–11.41)	100>CC$_{50}$ > 50	>5	3.87	56.85	4.35
1b [22]	Ar$_1$	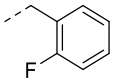	6.86 (6.03–7.77)	80.50 (67.65–113.9)	12	3.51	69.74	4.57
2b	Ar$_2$		1.13 (1.00–1.26)	50>CC$_{50}$ > 25	>22	4.92	69.74	3.62
3b	Ar$_3$		8.28 (7.14–9.60)	100>CC$_{50}$ > 50	>6	4.01	56.85	4.08
1c [22]	Ar$_1$	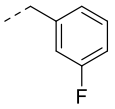	3.04 (2.69–3.41)	64.77 (53.46–80.16)	21	3.51	69.74	4.57
2c	Ar$_2$		3.07 (2.60–3.63)	>50	>16	4.92	69.74	3.62
3c	Ar$_3$		10.28 (9.04–11.68)	100>CC$_{50}$ > 50	>5	4.01	56.85	4.08
1d [22]	Ar$_1$	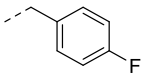	3.82 (3.29–4.43)	65.20 (52.13–87.97)	17	3.51	69.74	4.57
2d	Ar$_2$		2.38 (1.98–2.86)	50>CC$_{50}$ > 25	>11	4.92	69.74	3.62
3d	Ar$_3$		8.17 (7.09–9.41)	>50	>6	4.01	56.85	4.08
1e [22]	Ar$_1$	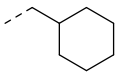	2.41 (2.16–2.69)	64.16 (54.50–76.87)	27	3.76	69.74	4.41
2e	Ar$_2$		1.44 (1.30–1.58)	100>CC$_{50}$ > 25	>17	5.07	69.74	3.67
3e	Ar$_3$		3.66 (3.28–4.08)	100>CC$_{50}$ > 50	>14	4.26	56.85	4.05
1f [22]	Ar$_1$	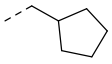	5.66 (4.93–6.46)	>100	>18	3.31	69.74	4.96
2f	Ar$_2$		1.41 (1.29–1.55)	100>CC$_{50}$ > 50	>35	4.65	69.74	3.95
3f	Ar$_3$		3.86 (3.53–4.21)	100>CC$_{50}$ > 50	>13	3.82	56.85	4.46
1g [22]	Ar$_1$		5.01 (4.24–5.89)	>100	>20	2.87	69.74	5.44
2g	Ar$_2$		1.88 (1.68–2.11)	100>CC$_{50}$ > 50	>27	4.23	69.74	4.26
3g	Ar$_3$		5.32 (4.71–6.00)	100>CC$_{50}$ > 50	>9	3.37	56.85	5.00
1h [22]	Ar$_1$		2.73 (2.46–2.98)	>100	>37	2.42	69.74	5.76
2h	Ar$_2$		0.89 (0.75–1.05)	50>CC$_{50}$ > 25	>28	3.81	69.74	4.66
3h	Ar$_3$		0.87 (0.81–0.93)	100>CC$_{50}$ > 50	>57	2.93	56.85	5.51
1i [22]	Ar$_1$		6.76 (5.19–8.56)	>100	>15	2.89	69.74	5.51
2i	Ar$_2$		1.95 (1.58–2.41)	>25	>13	4.28	69.74	4.32
3i	Ar$_3$		4.90 (4.18–5.74)	100>CC$_{50}$ > 50	>10	3.39	56.85	5.07
1l [22]	Ar$_1$	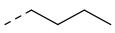	4.57 (3.98–5.28)	>100	>22	2.97	69.74	5.47
2l	Ar$_2$		1.89 (1.61–2.23)	100>CC$_{50}$ > 50	>26	4.31	69.74	4.30
3l	Ar$_3$		6.11 (5.42–6.89)	>100	>16	3.47	56.85	4.99

Data depicted are the calculated IC$_{50}$ and associated 95 % confidence interval from the merged data sets from at least three independent experiments for *T. brucei*; the CC$_{50}$ and associated 95 % confidence interval from the merged data sets from at least three independent experiments for THP-1 cells; Selectivity index (SI): IC$_{50}$ toward the parasite compared with compound cytotoxicity IC$_{50}$ on host cells (CC$_{50}$/IC$_{50}$).

[a] Marvin/JChem 20.9 was used to calculate logP (partition coefficient) values, topological polar surface area (TPSA, Å^2), and CNS multiparameter optimization (CNS MPO) values; ChemAxon (https://www.chemaxon.com).

kinetoplastid parasite. We carried out a phenotypic assay on *L. infantum* and *L. tropica* promastigotes exploiting the MTT (3-(4,5-dimethylthiazol-2-yl)-2,5-diphenyltetrazolium bromide) assay [30]. *L. infantum* is the etiologic agent of visceral leishmaniasis, whereas *L. tropica* causes CL. Unlike what is observed with other classes of compounds, we previously reported that the inhibition by 1,3,4-oxadiazoles of the free living and easily cultured promastigote stage correlates well with the inhibition of the clinically relevant but difficult to culture intra-macrophage amastigote stage [22]. Similarly to the data obtained for *T. brucei*, the 1,2,4-oxadiazoles (Ar$_2$, Table 2) proved to be more potent than the corresponding 1,3,4- regioisomers (Ar$_1$) when tested towards *Leishmania* spp. (Table 2). All 1,2,4 isomers displayed single digit micromolar activity against both *L. infantum* and *L. tropica*, with the cyclohexyl (**2e**), cyclopentyl (**2f**) and cyclobutyl (**2g**) substituted derivatives emerging as the most potent molecules (Table 2). The highest SI was obtained for compounds **2f** and **2g** (SI > 17). In conclusion, 1,2,4-oxadiazoles with cyclopentyl and cyclobutyl groups exhibited the best potency and SI across both *Leishmania* species (**2f**: IC$_{50}$ *L. infantum* = 3.01 μM, SI > 17; IC$_{50}$ *L. tropica* = 2.79 μM, SI > 18; **2g**: IC$_{50}$ *L. infantum* = 2.94 μM, SI > 17; IC$_{50}$ *L. tropica* = 2.57 μM, SI > 19). Smaller substituents, such as cyclopropyl (**2h**) and isobutyl (**2i**), resulted in reduced efficacy and SI < 10. Similarly to the 1,3,4-oxadiazoles, also the oxazole derivatives (Ar$_3$) showed reduced activity against *Leishmania* spp compared to their 1,2,4-oxadiazole analogues, with the only exception of compound **3h**, whose potency is comparable to that of **2h**. Thus, the 1,2,4-oxadiazole was highlighted as the preferred scaffold to develop antileishmanial compounds.

Table 2
Comparison of antileishmanial activity of 1,3,4-, 1,2,4- oxadiazoles and oxazoles.

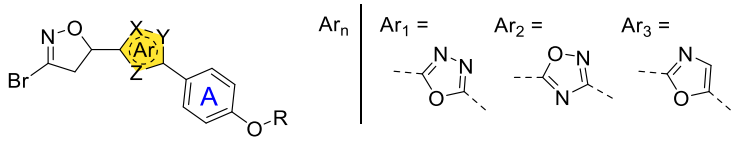

Comp.	Ar$_n$	R	*L. infantum*[a] IC$_{50}$ ± SD (μM)	CC$_{50}$ (μM) and (range)	SI	*L. tropica*[a] IC$_{50}$ ± SD (μM)	SI
1a [22]	Ar$_1$	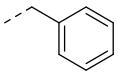	>40	>100	–	>40	–
2a	Ar$_2$		7.13 ± 1.85	100>CC$_{50}$ > 25	>4	5.61 ± 0.62	>4
3a	Ar$_3$		8.60 ± 1.05	100>CC$_{50}$ > 50	>6	18.30 ± 5.22	>3
1b [22]	Ar$_1$	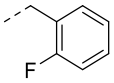	17.14 ± 6.41	80.5 (67.65–113.9)	5	24.73 ± 8.67	3
2b	Ar$_2$		4.93 ± 0.86	50>CC$_{50}$ > 25	>5	4.29 ± 0.06	>6
3b	Ar$_3$		12.81 ± 5.25	100>CC$_{50}$ > 50	>4	20.35 ± 6.63	>2
1c [22]	Ar$_1$	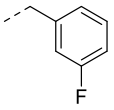	>40	64.77 (53.46–80.16)	–	>40	–
2c	Ar$_2$		5.78 ± 0.77	100>CC$_{50}$ > 50	>9	5.93 ± 0.91	>8
3c	Ar$_3$		11.83 ± 4.49	100>CC$_{50}$ > 50	>4	20.92 ± 1.38	>2
1d [22]	Ar$_1$	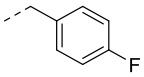	18.82 ± 10.47	65.20 (52.13–87.97)	4	29.93 ± 9.09	2
2d	Ar$_2$		5.41 ± 0.44	50>CC$_{50}$ > 25	>5	5.25 ± 0.18	>5
3d	Ar$_3$		15.55 ± 2.51	100>CC$_{50}$ > 50	>3	17.98 ± 1.06	>3
1e [22]	Ar$_1$	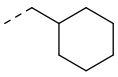	5.95 ± 1.56	64.16 (54.50–76.87)	11	8.98 ± 2.75	7
2e	Ar$_2$		2.72 ± 0.65	100>CC$_{50}$ > 25	>9	2.92 ± 0.30	>9
3e	Ar$_3$		18.08 ± 7.45	100>CC$_{50}$ > 50	>3	16.44 ± 1.53	>3
1f [22]	Ar$_1$	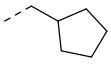	13.44 ± 5.16	>100	>7	20.24	–
2f	Ar$_2$		3.01 ± 0.81	100>CC$_{50}$ > 50	>17	2.79 ± 0.23	>18
3f	Ar$_3$		24.45 ± 2.50	100>CC$_{50}$ > 50	>2	13.33 ± 3.32	>4
1g [22]	Ar$_1$		10.63 ± 3.53	>100	>9	20.86 ± 8.30	>5
2g	Ar$_2$		2.94 ± 0.84	100>CC$_{50}$ > 50	>17	2.57 ± 0.52	>19
3g	Ar$_3$		21.46 ± 8.33	100>CC$_{50}$ > 50	>2	14.60 ± 2.55	>3
1h [22]	Ar$_1$		15.96 ± 4.38	>100	>6	26.19 ± 12.01	>4
2h	Ar$_2$		5.12 ± 0.93	50>CC$_{50}$ > 25	>5	4.31 ± 0.37	>6
3h	Ar$_3$		4.33 ± 1.01	>50	>12	6.35 ± 2.06	>8
1i [22]	Ar$_1$		>40	>100	–	>40	–
2i	Ar$_2$		3.49 ± 0.52	50>CC$_{50}$ > 25	>7	3.07 ± 0.05	>8
3i	Ar$_3$		>40	100>CC$_{50}$ > 50	>1	>40	>1
1l [22]	Ar$_1$		13.99 ± 5.53	>100	>7	20.76 ± 4.33	>5
2l	Ar$_2$		3.94 ± 0.06	100>CC$_{50}$ > 50	>13	3.68 ± 0.12	>14
3l	Ar$_3$		23.14 ± 10.35	>100	>4	40.22 ± 12.63	>2

[a] Data represent mean ± standard deviation of three independent experiments. *Leishmania* spp. (*L. infantum* and *L. tropica*) promastigotes were used. The CC$_{50}$ and associated 95 % confidence interval from the merged data sets from at least three independent experiments for THP-1 cells. Selectivity index (SI): IC$_{50}$ toward the parasite compared with compound cytotoxicity IC$_{50}$ on host cells (CC$_{50}$/IC$_{50}$).

3.3. Evaluation of anti-plasmodial activity

The *in vitro* activities of the novel 1,2,4-oxadiazoles and oxazoles libraries were determined against *P. falciparum* parasites and compared to those of the previously reported 1,3,4-oxadiazole derivatives [22]. We evaluated the antiplasmodial activity against multiple *P. falciparum* strains using two different assay readouts: the metabolic parasite lactate dehydrogenase (pLDH) assay after 72 h drug exposure, and the proliferation SYBR Green I assay with a 96 h drug exposure (covering two 48 h replication life cycles) [31,32]. The known antimalarial drug, chloroquine (CQ), was used as a reference activity across both assay readouts (Table 3). Data from these two readouts showed a positive correlation ($R^2 = 0.6$) as determined by a Pearson correlation coefficient (GraphPad Prism V8.0). Both assays were performed on well-characterized, genotyped drug sensitive and resistant *P. falciparum* strains. For the pLDH assay, the CQ-sensitive *Pf*D10 and CQ-resistant *Pf*W2 strains were used. For the SYBR Green I assay, the drug-sensitive *Pf*NF54 and -resistant *Pf*K1 and *Pf*Dd2 strains were used (Table 3). The *Pf*K1 and *Pf*Dd2 strains are genetically validated with point mutations in the CQ resistance transporter (*pfcrt)* and multidrug resistance 1 (*pfmdr1*), which confer resistance to CQ and amodiaquine. In addition, these also contain point mutations in the dihydrofolate reductase gene (*pfdhfr*), conferring resistance to pyrimethamine and cycloguanil, as well as the dihydropteroate synthase (*pfdhps*), conferring resistance to sulfadoxine [33]. The *Pf*Dd2 strain contains 3 copies of *pfmdr1* gene, in contrast to a single copy present in *Pf*K1 parasites. Therefore, cross-resistance screening

Table 3
In vitro activity of 1,3,4-oxadiazoles (**1a-1l**) 1,2,4-oxadiazoles (**2a-2l**) and oxazoles (**3a-3l**) against drug sensitive and drug resistant *P. falciparum* parasites.

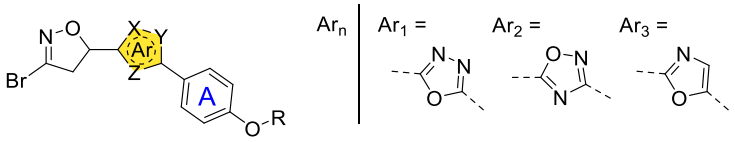

Comp.	Ar$_n$	R	pLDH							SYBR Green I			
			D10[a] IC$_{50}$ ± SD (μM)	CC$_{50}$ (μM) and range	SI	W2[a] IC$_{50}$ ± SD (μM)	SI	RI	NF54[b] IC$_{50}$ ± SEM (μM)	K1[b] IC$_{50}$ ± SEM (μM)	RI	Dd2[b] IC$_{50}$ ± SEM (μM)	RI
CQ			0.02 ± 0.00			0.27 ± 0.08		13.5	0.01 ± 0.00	0.16 ± 0.015	16.0	0.21 ± 0.00	21
1a [22]	Ar$_1$	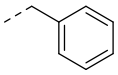	0.31 ± 0.05	>100	>326	0.40 ± 0.06	>252	1.3	0.22 ± 0.18	1.71 ± 0.19	7.8	1.33 ± 0.31	0.61
2a	Ar$_2$		9.05 ± 0.18	100>CC$_{50}$ > 25	>3	15.50 ± 0.68	>3	1.7	>5	ND	ND	ND	ND
3a	Ar$_3$		1.96 ± 0.37	100>CC$_{50}$ > 50	>26	4.41 ± 1.74	>11	2.3	1.11 ± 0.51	1.82 ± 0.15	1.6	2.22 ± 0.54	2.0
1b [22]	Ar$_1$	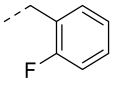	0.18 ± 0.04	80.50 (67.65–113.9)	460	0.23 ± 0.05	356	1.3	0.25 ± 0.09	0.67 ± 0.03	2.7	0.75 ± 0.71	3.0
2b	Ar$_2$		5.85 ± 0.42	50>CC$_{50}$ > 25	>4	10.13 ± 0.10	>2	1.7	>5	ND	ND	ND	ND
3b	Ar$_3$		0.87 ± 0.12	100>CC$_{50}$ > 50	>58	1.96 ± 0.64	>26	2.7	0.58 ± 0.15	0.98 ± 0.15	1.7	0.96 ± 0.29	1.6
1c [22]	Ar$_1$	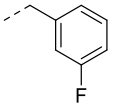	0.30 ± 0.08	64.77 (53.46–80.16)	220	0.35 ± 0.04	187	1.2	0.33 ± 0.09	1.22 ± 0.17	3.7	1.37 ± 0.15	4.2
2c	Ar$_2$		7.56 ± 0.28	>50	>13	12.37 ± 1.20	>8	1.6	>5	ND	ND	ND	ND
3c	Ar$_3$		2.87 ± 0.17	100>CC$_{50}$ > 50	>17	5.47 ± 1.94	>9	1.9	1.08 ± 0.03	2.62 ± 0.36	2.4	2.15 ± 0.73	2.0
1d [22]	Ar$_1$	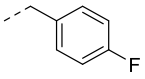	0.26 ± 0.03	65.20 (52.13–87.97)	248	0.31 ± 0.01	214	1.2	0.28 ± 0.81	0.41 ± 0.31	1.4	0.36 ± 0.05	1.3
2d	Ar$_2$		6.51 ± 0.43	50>CC$_{50}$ > 25	>4	10.30 ± 0.03	>2	1.6	>5	ND	ND	ND	ND
3d	Ar$_3$		1.67 ± 0.22	>50	>30	3.44 ± 1.31	>15	2.1	0.90 ± 0.08	1.21 ± 0.29	1.3	1.44 ± 0.37	1.6
1e [22]	Ar$_1$	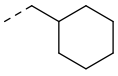	0.12 ± 0.04	64.16 (54.50–76.87)	553	0.16 ± 0.02	417	1.3	0.07 ± 0.02	0.20 ± 0.01	3.1	0.10 ± 0.00	1.5
2e	Ar$_2$		2.29 ± 0.03	100>CC$_{50}$ > 25	>11	4.44 ± 0.61	>6	1.9	>5	ND	ND	ND	ND
3e	Ar$_3$		0.60 ± 0.01	100>CC$_{50}$ > 50	>84	1.31 ± 0.20	>38	2.2	0.31 ± 0.03	0.55 ± 0.03	1.8	0.37 ± 0.12	1.2
1f [22]	Ar$_1$	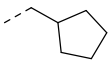	0.15 ± 0.04	>100	>658	0.22 ± 0.06	>458	1.4	0.10 ± 0.19	0.67 ± 0.07	6.5	0.37 ± 0.09	3.6
2f	Ar$_2$		5.69 ± 0.27	100>CC$_{50}$ > 50	>9	12.90 ± 0.48	>4	2.3	>5	ND	ND	ND	ND
3f	Ar$_3$		0.53 ± 0.14	100>CC$_{50}$ > 50	>94	1.16 ± 0.26	>43	2.2	0.21 ± 0.02	0.71 ± 0.03	3.4	0.44 ± 0.13	2.1
1g [22]	Ar$_1$	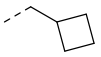	0.17 ± 0.08	>100	>581	0.23 ± 0.03	>441	1.3	0.22 ± 0.64	0.82 ± 0.03	3.7	0.84 ± 0.19	3.8
2g	Ar$_2$		8.81 ± 0.02	100>CC$_{50}$ > 50	>6	15.35 ± 2.72	>3	0.2	>5	ND	ND	ND	ND
3g	Ar$_3$		0.84 ± 0.18	100>CC$_{50}$ > 50	>60	1.77 ± 0.48	>28	2.1	0.48 ± 0.09	1.70 ± 0.32	3.5	2.06 ± 0.44	4.3
1h [22]	Ar$_1$		0.47 ± 0.04	>100	>213	0.58 ± 0.03	>173	1.2	0.57 ± 0.19	5.70 ± 0.65	10.0	6.17 ± 1.36	10.9
2h	Ar$_2$		16.15 ± 0.12	50>CC$_{50}$ > 25	>2	>20	>1	1.2	>5	ND	ND	ND	ND
3h	Ar$_3$		2.04 ± 0.02	>50	>25	5.66 ± 1.79	>9	2.8	2.48 ± 0.29	6.47 ± 0.77	2.6	3.78 ± 0.40	1.5
1i [22]	Ar$_1$		0.13 ± 0.03	>100	>769	0.22 ± 0.06	>459	1.7	0.18 ± 0.06	1.02 ± 0.02	5.7	0.94 ± 0.19	5.3
2i	Ar$_2$		8.67 ± 0.74	>25	>3	16.26 ± 7.36	>2	1.9	>5	ND	ND	ND	ND
3i	Ar$_3$		0.62 ± 0.07	100>CC$_{50}$ > 50	>81	2.76 ± 0.61	>18	4.5	0.28 ± 0.022	2.04 ± 0.30	7.4	1.20 ± 0.38	4.3
1l [22]	Ar$_1$	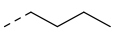	0.19 ± 0.03	>100	>526	0.30 ± 0.04	>332	0.1					
2l	Ar$_2$		9.42 ± 2.68	100>CC$_{50}$ > 50	>5	16.33 ± 6.06	>3	1.7	>5	ND	ND	ND	ND
3l	Ar$_3$		3.37 ± 0.28	>100	>30	7.91 ± 0.95	>13	2.3	0.62 ± 0.13	2.15 ± 0.28	3.5	4.21 ± 0.89	6.8

[a] Data represent mean ± S.D. or.

[b] mean ± S.E. of three independent experiments, each performed in technical duplicates. Chloroquine (CQ) was used as positive control. The CC_{50} and associated 95 % confidence interval from the merged data sets from at least three independent experiments for THP-1 cells. Selectivity index (SI): IC_{50} for parasite: compound cytotoxicity IC_{50} on host cells (CC_{50}/IC_{50}). Resistance index (RI): IC_{50} for *Pf*W2/*Pf*D10, *Pf*K1/*Pf*NF54 and *Pf*Dd2/*Pf*NF54. Not Determined (ND).

against these two strains allowed us to point out drug susceptibility linked to specific resistance mechanisms. A shift in drug susceptibility towards the *Pf*Dd2 strain suggests the involvement of a multidrug resistance 1 (MDR1) mediated resistance mechanism.

Compared to the 1,3,4-oxadiazoles (Ar_1), the 1,2,4 regioisomers (Ar_2, **2a-2l**) demonstrated negligible anti-plasmodial activity, with IC_{50} values greater than 5 μM against both drug sensitive and resistant *P. falciparum* strains in both assays (Table 3). Only the cyclohexyl substituted derivative **2e** (IC_{50} *Pf*D10 = 2.29 μM, *Pf*W2 = 4.44 μM) showed marginal micromolar activity in the pLDH assay. Similarly, **1e** and **3e** were also the most active molecules in their respective libraries, showing nanomolar activities against drug-sensitive and-resistant lines (Table 3). The oxazole derivatives showed variable anti-plasmodial activity in the micromolar to nanomolar range, with an average 6-fold reduction in activity compared to the 1,3,4-oxadiazole series. Notably, the oxazole ortho-*F*-benzyl derivative (**3b**) and the alkyl-substituted compounds (**3e-3g**, and **3i**) retained good activity against *P. falciparum* drug-sensitive (*Pf*NF54 and *Pf*D10) with IC_{50} values below 1 μM (Table 3). Indeed, considering the aryl-substituted molecules, the ortho-*F*-benzyl derivative was the most active derivative for both the 1,3,4-oxadiazole and oxazole libraries, showing nanomolar activities against drug-sensitive and resistant strains (see **1b** and **3b**, Table 3).

The oxazole derivatives shared the same SARs as the 1,3,4-oxadiazoles. Considering the aliphatic subgroup, the activity increased with the size of the cycloalkyl substituent (from 3 to 6-carbon atoms), with the cyclohexyl (**1e** and **3e**) and cyclopentyl (**1f** and **3f**) derivatives being the most potent. In parallel, the branched iso-butyl substituent (**1i** and **3i**) was preferred to the linear *n*-butyl (**1l** and **3l**, Table 3). Despite the oxazoles retaining activity, these results suggest that the 1,3,4-oxadiazole core remains the lead framework for anti-malarial drug development.

We observed negligible loss of compound activity due to *Pf*CRT and *Pf*MDR resistance indicators across all three resistant strains for all three libraries (see Table 3 data on avg RI *Pf*W2 = 2.5, *Pf*K1 = 2.9 and *Pf*Dd2 = 2.8) compared to the reference resistance indices (RI) for CQ (RI *Pf*W2 = 13.5, *Pf*K1 = 15.7 and *Pf*Dd2 = 21.6). For example, **3e** and **3f**, which are two of the most active compounds against drug sensitive lines on the SYBR Green I and pLDH (**3e**: 0.31 μM and 0.60 μM, **3f**: 0.21 μM and 0.53 μM) readouts retained activity across both resistant lines, with <2-fold change in IC_{50} values (see Table 3). The only exception being compounds **3g** and **3i**, with good activities against drug sensitive cell-lines (**3g**: 0.48 μM and **3i**: 0.84 μM), with >3-fold loss in activity for both *Pf*K1 and *Pf*Dd2 resistant strains, indicating marginal cross-resistance (see Table 3).

As a first line indication of the ability of these compounds to block *P. falciparum* parasite transmission, their activity against a 95 % synchronized stage IV to V gametocyte population [late stage gametocytes (lGc), >95 % IV-V] was evaluated using a transgenic luciferase reporter line, producing luciferase under a constitutive gametocyte specific promoter [34,35]. The observed inhibition of gametocyte viability was <30 % at 5 μM, indicating that these compounds have no transmission blocking potential (see Table S1, Supporting Information). However, determination of their activity against immature or mature gametocytes or gamete stages remains to be evaluated.

3.4. Reversibility assay in T. brucei for selected compound 3h

Our scaffold hopping approach allowed us to transform pan-active antiparasitic agents into a parasite-selective molecule (**3h**), targeting *T. brucei* parasites. As a final aspect of **3h** anti-*T. brucei* activity, we evaluated the irreversibility of the anti-parasitic effect (Fig. 2 and Table 4). We demonstrated that 8 h exposure was sufficient to induce significant irreversible effects, with the IC_{50} being 1.8-fold the 72 h IC_{50} (Table 4). Significantly, the anti-parasitic activity after 12 h of exposure was similar to that after 72 h. Using a similar approach for pentamidine, an 8 h exposure resulted in an anti-parasitic activity of 6-fold the 72 h IC_{50}. Moreover, a 24 h exposure to pentamidine, resulted in anti-parasitic activity that was still 1.9-fold the 72 h IC_{50}.

3.5. Early drug discovery pharmacological liability characterization

Compounds were characterized in a panel of early drug discovery pharmacological liability assays. This included cytotoxicity (A549 and HEK293 cell-lines) with 24 h compound incubation, metabolism (CYP3A4) and cardiotoxicity (*h*ERG). Compounds were screened in each assay to determine their % Effect at 10 μM and a traffic light system (Table 5) was used to rank compounds, as it allows for easy visualization and rapid decision making for SAR study and compound selection for progression. All tested compounds did not exhibit cytotoxicity against A549, with four compounds (**2b**, **2e**, **2g** and **2l**) associated with moderate cytotoxicity against HEK293. With regards to the metabolic profile of compounds, three compounds (**2g**, **3g** and **3h**) are associated with moderate/undesirable inhibition of CYP3A4. Finally, ten compounds are associated with moderate cardiotoxicity (*h*ERG). When considering the efficacy results and early drug discovery pharmacological liability characteristics, **2f** and **2g** are the best anti-Leishmanial agents, with the

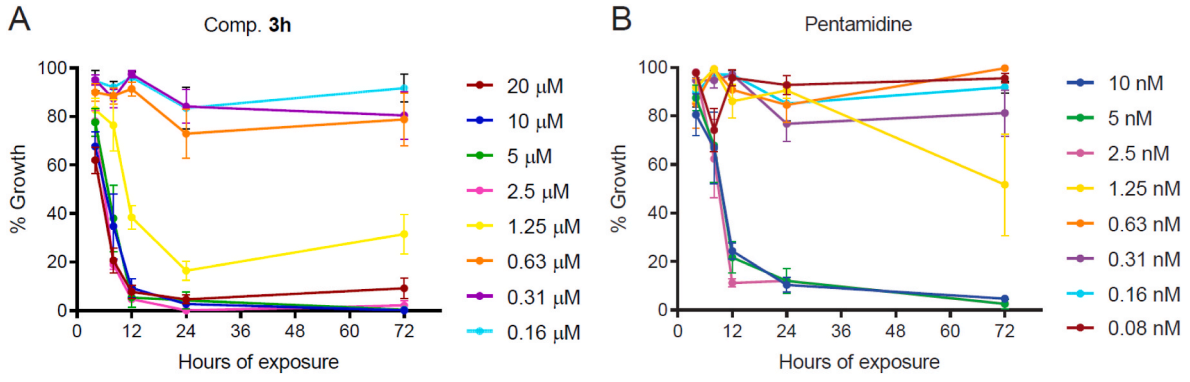

Fig. 2. *In vitro* irreversibility of *T. brucei* growth inhibition by **3h** (A) and pentamidine (B). Parasites were exposed to the drugs at specific concentrations for the time indicated, then were sedimented by centrifugation and resuspended in drug-free media. Parasite viability was measured at 72 h post-media change by the resazurin method. Data represented in each time point is the average and SEM of at least two independent assays performed in triplicate.

Table 4
In vitro irreversibility of *T. brucei* growth inhibition by **3h**.

		Time of exposure (h)				
		4	8	12	24	72
3h	IC_{50} μM (95 % CI)	23.92 (15.50–36.90)	1.78 (1.60–1.98)	1.26 (1.15–1.39)	0.88 (0.82–0.93)	0.97 (0.88–1.08)
Pentamidine	IC_{50} nM (95 % CI)	–	13.55 (9.60–19.13)	5.88 (4.68–7.39)	4.39 (3.70–5.21)	2.27 (1.70–3.04)

Table 5
Early drug discovery pharmacological liability characterization of compounds.

Comp.	% Cytotoxicity A549	% Cytotoxicity HEK293	% CYP3A4 Inhibition	% *h*ERG Inhibition
1a	12	10	31	18
2a	-1	36	2	23
3a	-1	-4	-1	52
2b	7	63	-1	55
3b	13	20	1	38
2c	5	15	0	42
3c	-6	-11	0	62
1d	3	3	31	13
2d	9	20	0	39
3d	-6	-2	0	35
1e	15	4	25	50
2e	8	62	0	52
3e	-9	-2	0	73
2f	21	18	0	36
3f	0	6	18	72
1g	8	9	19	26
2g	18	64	83	58
3g	-21	9	91	57
1h	21	15	22	10
2h	10	34	92	9
3h	-6	19	-1	50
1i	20	18	31	15
2i	3	19	22	13
3i	9	46	-1	34
1l	11	10	41	24
2l	12	68	0	36
3l	-3	-2	2	21

All assays were performed at 10 μM compound concentration. The data are reported as a traffic light system: Green = preferred criteria (<50 % Inhibition at 10 μM compound concentration), yellow = moderate inhibition (51–89 % Inhibition at 10 μM compound concentration) and red = undesirable inhibition (>900 % Inhibition at 10 μM compound concentration). All assay plates passed quality control assessment with Z′ value for each assay plate being a minimum value of 0.6. All experiments were performed in independent duplicate, and <10 % standard error for each % Inhibition.

former having a significantly better early drug discovery pharmacological liability profile. With regards to antiplasmodial activity, **3e** and **3f** are the best compounds from the novel series, and display a similar safety profile when compared to the 1,3,4-oxadizoles previously published (**1e** vs. **3e**). As for *T. brucei*, the best molecule **3h** is not cytotoxic, does not inhibit CYP3A4, although there is moderate *h*ERG inhibition.

4. Conclusion

We previously demonstrated that the 1,3,4-oxadiazole is a privileged scaffold for the development of pan-active antiparasitic agents [22]. Through a scaffold-hopping approach, we replaced the 1,3,4-oxadiazole core with its regioisomer, a 1,2,4-oxadiazole core, or with the oxazole ring. As a general trend, we observed that the 1,2,4-oxadiazoles showed higher anti-*T. brucei* and anti-*Leishmania* potencies compared to their

corresponding 1,3,4 regioisomers, whereas they displayed a significant decrease in anti-plasmodial activity. On the other hand, the 1,3,4-oxadiazole scaffold proved to be the best choice to obtain potent anti-plasmodial activity, followed by the oxazole core (Fig. S2).

All 1,2,4 isomers displayed a single digit micromolar activity against both *L. infantum* and *L. tropica*, with the cyclopentyl- (**2f**) and cyclobutyl- (**2g**) substituted derivatives emerging as the most potent and selective anti-leishmanial agents. According to early drug discovery pharmacological liability characterization, **2f** displayed a safety profile, while **2g** presented several liabilities (moderate cytotoxicity against HEK293, moderate/undesirable inhibition of CYP3A4 and moderate cardiotoxicity). Compounds **2f** and **2g** also displayed significant activity towards *T. brucei*, with IC_{50} values lower than 2 μM and SI > 25, thus being pan-kinetoplastid agents. However, their high lipophilicity resulted in CNS MPO scores <5, decreasing their likelihood of potential application in stage 2 HAT treatment. The oxazole derivatives generally exhibited reduced anti-kinetoplastid activity compared to their 1,2,4-oxadiazole counterparts while being significantly more active as anti-plasmodial agents, although still less potent than their 1,3,4-oxadiazole analogues. Among the novel oxazole series, the cyclohexyl- and cyclopentyl-substituted compounds, **3e** and **3f** were the only derivatives showing nM activity against both drug sensitive (*Pf*D10 and *Pf*Nf54) and resistant (*Pf*W2, *Pf*K1 and *Pf*Dd2) *P. falciparum* parasites, as validated across a metabolic and proliferative readout. The cyclopropyl-substituted oxazole **3h**, displaying modest antiplasmodial activity, was identified as the most potent and selective anti-*T. brucei* agent (IC_{50} = 0.87 μM; SI > 57) showing desirable physicochemical properties for BBB penetration (*CNS MPO* >5) and early drug discovery pharmacological liability characteristics. Compound **3h** also presented a low micromolar IC_{50} value towards *Leishmania* spp, although in this case the SI for parasite versus human cells is reduced (SI < 15, Table 2). Overall, **3h** possesses a promising profile as antitrypanosomal agent, and the reversibility data suggest that an 8 h exposure is sufficient to cause irreversible damage to the *T. brucei* parasites. This property is most relevant in conjunction with pharmacokinetic data, to evaluate if these molecules have the potential to be active *in vivo* in murine models of infection enabling the design of optimal therapeutic approaches. It is expected that at least 8 h exposure to plasma concentrations higher than the 2-fold IC_{50} of **3h** will be required for *in vivo* anti-parasitic activity. Overall, the *in vitro* data generated for **3h** provides a solid background for future evaluation of its potential as an anti-trypanosomal lead.

5. Experimental section

5.1. Chemistry section

Reagents were purchased at the highest commercial quality from Sigma-Aldrich or Fluorochem and used without further purification. DBF was prepared according to literature [28]. ^{1}H NMR and ^{13}C NMR spectra were recorded with a Varian Mercury 300 (300 MHz) spectrometer. NMR spectra were obtained in deuterated solvents, $CDCl_3$, methanol-d_4 and DMSO-d_6. The chemical shift (δ values) are reported in ppm and corrected to the signal of the deuterated solvents [7.26 ppm (^{1}H NMR) and 77.16 ppm (^{13}C NMR) for $CDCl_3$; 2.50 ppm (^{1}H NMR) and 39.52 ppm (^{13}C NMR) for DMSO-d_6; and 3.31 ppm (^{1}H NMR) and 49.00 ppm (^{13}C NMR) for methanol-d_4]. Peak multiplicities are reported as: s (singlet), d (doublet), dd (doublet of doublets), t (triplet), dt (doublet of triplets), q (quartet), m (multiplet), br (broadened). Chemical shifts (δ) are expressed in ppm and coupling constants (J) in Hertz (Hz). Thin layer chromatography (TLC) plates were purchased from Sigma-Aldrich (silica gel 60 $F^{25}4$ aluminum sheets, with fluorescence indicator 254 nm) and UV light (254 nm) was used to visualize the compounds. Flash chromatography was performed using silica gel, pore size 60 Å, 230–400 mesh particle size. High-resolution mass spectrometry (HRMS) analyses were performed with the SYNAPT G2-Si QTof High Definition Mass Spectrometer or the Ultimate 3000 HPLC (Dionex), set to automatically inject into the LTQ Orbitrap XL mass spectrometer (Thermo Fisher Scientific, USA), operating in full scan mode. Analyses were carried out in positive ion mode. The chromatographic purity of final compounds was determined by high-performance liquid chromatography (HPLC) analyses on a Waters 1525 Binary HPLC Pump, equipped with a Waters 2489 UV–vis detector (Waters, Milford, MA), using a Symmetry C18 Column (4.6 × 75 mm^2, 3.5 μm particle size). Solvents A and B (A = Millipore water with 0.1 % TFA, B = ACN with 0.1 % TFA) and three different methods were used. Method A: gradient elution (85:15 for 0.2 min, 85:15 → 5:95 over 14 min) of the mobile phase consisting of solvents A and B at a flow rate of 1 mL/min at room temperature. Method B: gradient elution (40:60 for 0.2 min, 40:60 → 5:95 over 14 min) of the mobile phase consisting of solvents A and B at a flow rate of 1 mL/min at room temperature. Method C: gradient elution (60:40 for 0.2 min, 60:40 → 5:95 over 14 min) of the mobile phase consisting of solvents A and B at a flow rate of 1 mL/min at room temperature. The purity of all final compounds was >95 %.

5.1.1. General procedure 1

To a stirred 0.5 M solution of *p*-hydroxybenzaldehyde **4** (1.0 eq.) in acetone, the desired alkyl-/arylalkyl bromide (1.1 eq.) and K_2CO_3 (1.5 eq.) were added. The reaction mixture was heated at reflux overnight. After completion of the reaction monitored by TLC, the suspension was allowed to cool down to room temperature and then filtered to remove K_2CO_3. Acetone was removed under reduced pressure. The crude product was dissolved in EtOAc, the organic phase was washed with water (3x), dried over anhydrous Na_2SO_4, filtered and evaporated under reduced pressure to obtain compounds **5a-5e** and **5g-5l**. The crude was purified by column chromatography on silica gel.

5.1.2. General procedure 2

To a stirred solution of **5a-5l** (1.0 eq.) in pyridine (30.0 eq.), $NH_2OH{\cdot}HCl$ (2.0 eq.) was added. The reaction mixture was heated at 85 °C and, when the desired temperature was reached, Ac_2O (20.0 eq.) was added. The reaction was stirred at 85 °C for 2 h. After completion of the reaction monitored by TLC, the solution was allowed to cool down to room temperature, poured in water and extracted with EtOAc (3x). Then, the organic phase was washed with 2 M HCl (3x), dried over anhydrous Na_2SO_4, filtered and evaporated under reduced pressure to obtain compounds **6a-6l**. The crude was purified by column chromatography on silica gel.

5.1.3. General procedure 3

To a stirred 0.4 M solution of **6a-6l** (1.0 eq) in EtOH, a 3 M solution of $NH_2OH{\cdot}HCl$ (2.2 eq.) in H_2O and a 1.4 M solution of Na_2CO_3 (1.7 eq.) in H_2O were added. The reaction mixture was heated at reflux overnight. After completion of the reaction monitored by TLC, the suspension was allowed to cool down to room temperature and the solvent was evaporated under reduced pressure. The crude product was dissolved in EtOAc, the organic phase was washed with water (3x), dried over anhydrous Na_2SO_4, filtered and evaporated under reduced pressure. The crude product was triturated with diethyl ether and then filtered on a Buchner to obtain compounds **7a-7l**.

5.1.4. General procedure 4

A 0.2 M solution of **7a-7l** (1.0 eq.) in dry THF was cooled to 0 °C, then acryloyl chloride (1.5 eq.) was added dropwise. The reaction mixture was stirred at room temperature for 1–2 h. After completion of the reaction monitored by TLC, the reaction mixture was quenched with a 5 % aq. solution of $NaHCO_3$. The aqueous phase was extracted with

EtOAc (3x) and the organic layer was dried over anhydrous Na_2SO_4, filtered and evaporated under reduced pressure to obtain compounds **8a-8l**. The crude was purified by column chromatography on silica gel.

5.1.5. General procedure 5

To a stirred 0.1 M solution of **8a-8l** (1.0 eq.) in dry THF, 1 M TBAF (0.2 eq.) in dry THF was added. The reaction mixture was stirred for 2 h at room temperature. After completion of the reaction monitored by TLC, the reaction mixture was quenched with 2 M HCl. Then, the aqueous layer was extracted with EtOAc (3x), the organic phase was dried over anhydrous Na_2SO_4, filtered and concentrated under reduced pressure to obtain compounds **9a-9l**. The crude was purified by column chromatography on silica gel.

5.1.6. General procedure 6

To a 0.1 M solution of **9a-9l** (1 eq.) in EtOAc, $NaHCO_3$ (5 eq.) and DBF (1.5 eq.) were added. The reaction mixture was stirred overnight at room temperature. After completion of the reaction monitored by TLC, water was added and the aqueous layer was extracted with EtOAc (3x). Then, the organic phase was dried over anhydrous Na_2SO_4, filtered, and concentrated under reduced pressure to obtain compounds **2a-2l**. The crude was purified by flash chromatography on silica gel.

5.1.7. General procedure 7

To a 0.3 M solution of 4′-hydroxyacetophenone **10** (1.0 eq.) in acetone, solid K_2CO_3 (1.5 eq.) and the desired alkyl/arylalkyl bromide (1.1 eq) were added. The reaction mixture was heated at reflux overnight. After completion of the reaction, monitored by TLC, the mixture was filtered and the solvent was removed under reduced pressure. EtOAc was added and the organic phase was washed with a 0.5 N solution of NaOH (2x). The organic phase was dried over anhydrous Na_2SO_4, filtered and evaporated under reduced pressure to obtain compounds **11a-11e** and **11g-11l**, which were used without further purification unless specified.

5.1.8. General procedure 8

To a 0.1 M stirred solution of **11c-11i** (1.0 eq.) in chloroform at 0 °C, Br_2 (1.3 eq.) was added dropwise. The reaction mixture was stirred at room temperature for 1 h. After completion of the reaction monitored by TLC, the mixture was diluted with an aqueous solution of $Na_2S_2O_3$ and extracted with chloroform (3x). Then the organic phase was dried anhydrous Na_2SO_4, filtered and evaporated under reduced pressure to obtain compounds **12c-12i**. The crude was purified by flash chromatography on silica gel.

5.1.9. General procedure 9

Step 1: To a 0.2 M stirred solution of **12a-12l** (1.0 eq.) in 1,2-dichloroethane, hexamine (1.1 eq.) was added. The reaction mixture was stirred at 60 °C for 1 h. After completion of the reaction monitored by TLC, the suspension was allowed to cool down to room temperature, filtered and the precipitate was collected and suspended in MeOH. To the suspension, HCl_{conc} (4.0 eq.) was added dropwise, and the reaction mixture was stirred at reflux for 1 h. Afterwards, the suspension was allowed to cool down to room temperature and concentrated under reduced pressure to obtain compounds **13a-13l**, which were used for the next step without further purification.

Step 2: To a stirred 0.2 M solution of **13a-13l** (1.0 eq.) in dry DCM, acryloyl chloride (1.2 eq.) and Na_2CO_3 (10.0 eq.) were added. The reaction mixture was stirred at room temperature overnight. After completion of the reaction monitored by TLC, H_2O was added and the solution was stirred for 15 min, then the aqueous phase was extracted with DCM (3x) and the organic layer was dried over anhydrous Na_2SO_4, filtered and evaporated under reduced pressure to obtain compounds **14a-14l.** The crude was purified by column chromatography on silica gel.

5.1.10. General procedure 10

Step 1: To a stirred solution of **14a-14l** (1.0 eq.), $POCl_3$ (50.0 eq.) was added. The reaction mixture was heated at reflux overnight. After completion of the reaction monitored by TLC, the solution was allowed to cool down to room temperature, water was added and the aqueous phase was extracted with EtOAc (3x). Then, the organic phase was dried over anhydrous Na_2SO_4, filtered and evaporated under reduced pressure to obtain compounds **15a-15l**, which were used for the next step without further purification.

Step 2: To a stirred 0.1 M solution of **15a-15l** (1.0 eq.) in EtOAc, $NaHCO_3$ (5 eq.) and DBF (1.5 eq.) were added. The reaction mixture was stirred overnight at room temperature. After completion of the reaction monitored by TLC, H_2O was added and the aqueous layer was extracted with EtOAc (3x). Then, the organic phase was dried over anhydrous Na_2SO_4, filtered, and concentrated under reduced pressure to obtain compounds **3a-3l.** The crude was purified by flash chromatography on silica gel.

5.2. Biological section

5.2.1. Parasite cultures

T. b. brucei Lister 427 bloodstream forms were grown in a humidified incubator at 37 °C, 5 % CO_2 in complete HMI-9 medium 1 supplemented with 10 % heat-inactivated Fetal Bovine Serum (FBS) and 100 UI/mL penicillin/streptomycin. Parasites maintenance was done in T25 ventilated flasks by subpassage at a concentration of 1×10^4/mL every 2 days on T25 ventilated flasks.

Promastigote stage of *L. infantum* strain (MHOM/TN/80/IPT1, kindly provided by Dr. M. Gramiccia and Dr. T. Di Muccio, ISS, Roma) and *L. tropica* (MHOM/SY/2012/ISS3130) were cultured in RPMI 1640 medium (EuroClone) supplemented with 10 % heat-inactivated fetal calf serum (EuroClone), 20 mM Hepes, and 2 mM L-glutamine at 24 °C.

P. falciparum cultures were carried out according to Trager and Jensen with slight modifications [36]. The CQ-susceptible strains D10 and the CQ-resistant strain W2 were maintained at 5 % hematocrit (human type A-positive red blood cells) in RPMI 1640 (EuroClone) medium with the addition of 1 % AlbuMax (Invitrogen, Milan, Italy), 0.01 % hypoxanthine, 20 mM Hepes, and 2 mM glutamine. All the cultures were maintained at 37 °C in a standard gas mixture (1 % O_2, 5 % CO_2, and 94 % N_2). *Pf*NF54 (MRA-1000), *Pf*K1 (MRA-159) and *Pf*Dd2 (MRA-150) parasites were obtained through BEI resources (Malaria Research and Reference Reagent Resource Center, Manassas, USA), and maintained in similar conditions (RPMI-164 (Gibco), 0.5 % (w/v) Albumax II (Invitrogen), 20 mM HEPES, 0.2 mM hypoxanthine, 0.2 % (w/v) glucose, 23.81 mM sodium bicarbonate (Sigma-Aldrich) and 0.024 mg/mL gentamycin (Pharma-Q) at a 5 % haematocrit at 90 % N_2, 5 % CO_2 and 5 % O_2 [36].

5.2.2. Cell Cultures

Human leukemia cell line, THP-1 (ATCC® TIB-202™) were cultured in RPMI-1640 medium supplemented with 10 % heat-inactivated Fetal Bovine Serum (FBS), 2 mM L-glutamine, 100 UI/mL penicillin/streptomycin, 20 mM HEPES. The cell line was maintained in a humidified incubator at 37 °C and 5 % CO_2 by subculture every three days in 20 mL of media at a concentration of 1x105/ml in a T75 flask. All cell culture reagents were purchased from Lonza-Bioscience (Morrisville, NC).

5.2.3. In vitro evaluation of anti-T. brucei activity

The efficacy of compounds against *T. brucei brucei* bloodstream forms was evaluated using a modified resazurin-based assay previously described in literature [2,37]. Parasites were added to 100 μL of serial dilutions of compounds in supplemented complete medium at a cell density of 5×10^3/mL. As a quality control, a dose response curve for the antitrypanosomal pentamidine was included in all the assays. The final volume of the assay is 200 μL/well. Each condition was carried out in duplicate. Following 72h incubation at the specific conditions for each

parasite, 20 μL of a 0.5 mM resazurin solution was added and plates were incubated for a further 4 h under the same conditions. Fluorescence was measured at 544 nm and 590 nm excitation and emission wavelength, respectively, using a Synergy 2 Multi-Mode Reader (Biotek, Winooski, VT, USA). Results were shown as % of parasite growth inhibition compared to control (untreated parasites) and represent the average of at least three independent experiments. The effect was evaluated by the determination of the IC_{50} value (concentration required to inhibit growth in 50 %) and calculated by non-linear regression curves using GraphPad Prism version 8.1.1 for Windows (GraphPad Software, San Diego CA, USA). For the reversibility assay the assay is similar to what is described above with the following modification, the parasites were exposed to the defined concentrations of drug in a U bottom plate, at defined times the plates were centrifuged twice at 1800g for 5 min, and suspended in media without drugs. The assay follows then as described above.

5.2.4. Antileishmanial activity assay

To estimate the 50 % inhibitory concentration (IC_{50}) towards *L. infantum* strain (MHOM/TN/80/IPT1) and *L. tropica* (MHOM/SY/2012/ISS3130) promastigotes, the MTT (3-[4.5-dimethylthiazol-2-yl]-2.5-diphenyltetrazolium bromide) method was used [38]. Compounds were dissolved in DMSO and then diluted with medium to achieve the required concentrations. Drugs were placed in 96 wells round-bottom microplates and seven serial dilutions made. Parasites were diluted in complete medium to 5×10^6 parasites/mL and 100 μL of the suspension was seeded into the plates, incubated at 24 °C for 72 h and then 20 μL of MTT solution (5 mg/mL) was added into each well for 3 h. The plates were then centrifuged at 1000×*g* for 8 min at r.t., the supernatants discarded and the resulting pellets dissolved in 100 μL of lysing buffer consisting of 20 % (w/v) of a solution of SDS (Sigma), 40 % of DMF (Merck) in H_2O. The absorbance was measured spectrophotometrically at a test wavelength of 550 nm and a reference wavelength of 650 nm. The results are expressed as IC_{50} which is the dose of compound necessary to inhibit parasite growth by 50 %; each IC_{50} value is the mean of separate experiments performed in duplicate.

5.2.5. Antimalarial activity assay using pLDH assay

All compounds were dissolved in DMSO and then diluted with medium to achieve the required concentrations (final DMSO concentration <1 %, non-toxic to the parasite). Drugs were placed in 96-well flat-bottomed microplates (Corning-Costar) and serial dilutions made. Asynchronous cultures with parasitaemia of 1–1.5 % and 1 % final hematocrit were aliquoted into the plates and incubated for 72 h at 37 °C. Parasite growth was determined spectrophotometrically (OD650) by measuring the activity of the parasite lactate dehydrogenase (pLDH), according to a modified version of the method of Makler in control and drug-treated cultures [39]. The antiplasmodial activity is expressed as 50 % inhibitory concentrations (IC_{50}); each IC_{50} value is the mean ± standard deviation of at least three separate experiments performed in duplicate.

5.2.6. SYBR green I anti-proliferative activity assay

Prior to assays parasites were synchronized to >95 % ring stages using 5 % (w/v) D-Sorbitol (Sigma-Aldrich) [40], with parasite proliferation being monitored microscopically through Giemsa-stained thin smears (Rapid-Diff, Clinical Sciences Diagnostics). Compounds were dissolved in 100 % DMSO (Sigma-Aldrich), with working solutions being prepared in complete culture media. Parasites at a 1 % parasitemia and 1 % hematocrit were treated for 96 h at 37 °C under hypoxic conditions (described above). Parasite proliferation was determined using the SYBR Green I assay [31]. Following incubation, parasites were lysed through addition of equal (v/v) amounts of a SYBR Green I lysis buffer (0.2 % μL/mL of 10 000x SYBR Green I (Thermo Fisher), 20 mM Tris-HCl, pH 7.5, 5 mM EDTA, 0.008 % saponin (*w/v*) and 0.08 % Triton x-100 (Sigma-Aldrich)). SYBR Green fluorescence as a proxy for DNA content was measured using a Fluoroskan Acsent FL (Thermo Labsystems) at 485/538 nm. Data were normalized to an untreated negative control, using the known antimalarial drug, choloroquine, as a positive antiproliferative control, and IC_{50} were determined using GraphPrism V8.0 software. Data are expressed as mean ± S.E., for three biological replicates ($n = 3$), each performed in technical duplicates.

5.2.7. In-vitro late-stage gametocyte activity determination

Stage-specific gametocytocidal action of 1,2,4-oxadiazoles and oxazoles was determined against late (>90 % stage IV–V) gametocytes using the *P. falciparum* luciferase reporter line, 3D7elo1-pfs16-CBG99 (kind gift from Pietro Alano, ISS, Italy), as previously described [41]. Drug assays were conducted at 1.5 % gametocytaemia and 2 % haematocrit for 48 h under drug pressure under hypoxic conditions (90 % N_2, 5 % O_2, and 5 % CO_2) at 37 °C, with methylene blue and MMV390048 serving as internal reference controls. The luciferase reporter assay was performed using 0.5 mM non-lysing D-luciferin (Regis Technologies) in citrate buffer (50 mM citric acid, 50 mM trisodium citrate hydrate) with bioluminescence detection using the GloMax®-Multi Detection System with Instinct® software. Inhibition *values* (%) were determined using GraphPad Prism V8 software (as described above) and expressed as the mean from a single biological repeat ($n = 1$) performed in technical triplicates.

5.2.8. Cytotoxicity in THP-1 cells

The cytotoxicity effect of compounds on THP-1-derived macrophages was assessed by the colorimetric MTT assay (3-(4,5-dimethylthiazol-2-yl)-2,5-diphenyl tetrazolium bromide). Briefly, THP-1 cells were suspended in RPMI complete medium at a density of 1x06 cells/mL and 100 μL/well were seeded in a 96-well plate and were differentiated into macrophages by addition of 40 ng/mL of phorbol-myristate 13-acetate (PMA, Sigma, Saint Louis, MI, USA) for 24 h followed by replacement with fresh medium for more 24 h. Subsequently, cells were incubated with 100 μL of compounds ranging from 100 to 12.5 μM after dilution in the RPMI complete medium. Each condition was carried out in quadruplicate. After 72 h of incubation at 37 °C 5 % CO_2, the medium was removed and 200 μL of 0.5 mg/mL MTT solution diluted in RPMI was added. Plates were incubated for an additional 4 h. Then 160 μL of media was removed and the same volume of 2-propanol was added. Absorbance was read at 570 nm using a Synergy 2 Multi-Mode Reader (Biotek, Winooski, VT, USA). Cytotoxicity was evaluated by the determination of the CC_{50} value (drug concentration that reduced the percentage of viable cells in 50 %) and calculated by non-linear regression analysis using GraphPad Prism version 8.1.1 for Windows (GraphPad Software, San Diego, CA, USA). The results represent the average of at least three independent experiments. For each compound, the Selectivity Index (SI) was calculated as the ratio between cytotoxicity in THP-1 (CC_{50}, 72 h) and activity against parasites (IC_{50}, 72 h).

5.2.9. Early drug discovery pharmacological liability characterization of compounds

These assays have been extensively employed for cytotoxicity (A549 and HEK293), CYP3A4 and hERG to profile compounds and the methodology has been previously described [22]. Assay Kits were utilized for these studies which included CellTiter-Glo reagent for cytotoxicity (G7572, Promega Corp., Madison, WI), Vivid CYP3A4 Green for CYP3A4 (P2857, ThermoFisher Scientific, Carlsbad, CA, USA), and Predictor *h*ERG based cardiotoxicity (PV5365, ThermoFisher Scientific, Carlsbad, CA, USA). Screening of compounds was performed in 384-well microtiter plates. A Cell Explorer HTS platform (PerkinElmer, Waltham, MA, USA) equipped with an Echo 550 Liquid Handler (Labcyte, Sunnyvale, CA, USA), Multidrop (ThermoFisher Scientific, Carlsbad, CA, USA) liquid handling system and EnVision Multilabel 2103 Reader (PerkinElmer, Waltham, MA, USA) were used for low-volume compound and bulk reagent addition and readout, respectively. The raw data from compounds of screening at 10 μM were analyzed using Excel (Microsoft,

Seattle, WA, USA). Raw data from each assay plate were normalized using the respective controls located in an entire column of each assay plate (0.1 % v/v DMSO yielding 0 % Inhibition in each assay; assay specific reference inhibitor in 0.1 % v/v DMSO yielding 100 % Inhibition in each assay). All assay plates underwent quality control assessment following calculation of the Z′ value for each assay plate with a minimum value of 0.6. The % Inhibition for each compound at 10 μM was calculated and reported. All experiments were performed in duplicate, and the standard error for each result (% Inhibition) was <10 %. A549 and HEK293 cell lines were from DSMZ, German Collection of Micro-organisms and Cell Cultures, Braunschweig, Germany.

Briefly, (1) cytotoxicity assays in luminescence readout determined the number of viable cells in culture based on quantitation of the ATP present, an indicator of metabolically active cells, (2) the CYP3A4 in fluorescence intensity readout made use of CYP3A4 BACULOSOMES® Plus reagent containing microsomes prepared from insect cells expressing a human P450 isozyme and a CYP3A4 specific substrate (Vivid® DBOMF Substrate), and (3) *h*ERG assay in fluorescence polarization readout made use of membrane fraction containing *h*ERG channel protein (Predictor™ *h*ERG Membrane) and a high-affinity red fluorescent *h*ERG channel ligand, or "tracer" (Predictor™ *h*ERG Tracer Red).

CRediT authorship contribution statement

Chiara Borsari: Writing – review & editing, Writing – original draft, Visualization, Supervision, Project administration, Methodology, Investigation, Formal analysis, Data curation, Conceptualization. **Nuno Santarem:** Writing – review & editing, Validation, Methodology, Formal analysis, Data curation. **Dina Coertzen:** Writing – review & editing, Validation, Methodology, Formal analysis, Data curation. **Asia Mazzolari:** Methodology, Investigation. **Alexandra Ioana Corfu:** Methodology, Investigation. **Catarina Coelho:** Methodology, Investigation. **Francisca Barbosa:** Methodology, Investigation. **Lucia Tamborini:** Validation, Methodology, Investigation. **Lyn-Marié Birkholtz:** Validation, Methodology, Investigation. **Lorenzo Raffellini:** Methodology, Investigation. **Oliver Keminer:** Validation, Methodology, Investigation. **Nicoletta Basilico:** Validation, Methodology, Investigation. **Silvia Parapini:** Validation, Methodology, Investigation. **Sheraz Gul:** Writing – review & editing, Supervision, Investigation, Formal analysis, Data curation. **Anabela Cordeiro-da-Silva:** Writing – review & editing, Supervision, Methodology, Investigation, Formal analysis, Data curation. **Paola Conti:** Writing – review & editing, Writing – original draft, Supervision, Methodology, Investigation, Formal analysis, Data curation.

Ethics statement

Parasitology work (University of Pretoria) was covered under ethical approval from the University of Pretoria Health Sciences Ethics Committee (506/2018) and Natural and Agricultural Sciences Ethics Committee (180000094).

Funding sources

C.B. and P.C. are grateful to the UNIMI GSA-IDEA project for financial support. N.S. is an assistant researcher funded by national funds through FCT and co-funded through the European Social Fund within the Human Potential Operating Programme with reference 2021.04285.CEECIND/CP1663/CT0004. The Department of Science and Innovation and the National Research Foundation South African Research Chair (SARChI) in Sustainable Malaria Control to L-M.B. (UID 84627).

Declaration of competing interest

The authors declare that they have no known competing financial interests or personal relationships that could have appeared to influence the work reported in this paper.

Acknowledgements

This publication is based upon work from COST Action CA21111 "One Health drugs against parasitic vector borne diseases in Europe and beyond (OneHealthdrugs)", supported by COST (European Cooperation in Science and Technology). We are grateful to the Immunohematology and Transfusion Medicine Service, Department of Laboratory Medicine, and ASST Grande Ospedale Metropolitano Niguarda (Milan) for providing the erythrocytes for parasite cultures. We are grateful to the Mass Spectrometry facility of the Unitech COSPECT at the University of Milan (Italy) for the mass spectrometry analyses.

Appendix A. Supplementary data

Supplementary data to this article can be found online at https://doi.org/10.1016/j.ejmech.2025.118095.

Abbreviations Used

ACN	acetonitrile;
BBB	blood brain barrier
CC_{50}	half-maximal cytotoxicity concentration
CNS	central nervous system
DCM	dichloromethane
DIPEA	*N*,*N*-diisopropylethylamine;
EtOH	Ethanol
G6PD	glucose-6-phosphate dehydrogenase
HAT	Human African Trypanosomiasis
HDAC	histone deacetylase
L. infantum	*Leishmania infantum*
PBS	phosphate-buffered saline;
P. falciparum	*Plasmodium falciparum*
THF	tetrahydrofuran
THP-1	human monocytic cell-line
T. brucei	*Trypanosoma brucei*
VBPDs	vector-borne parasitic diseases

Data availability

Data will be made available on request.

References

[1] M. Cholewiński, M. Derda, E. Hadaś, Parasitic diseases in humans transmitted by vectors, Ann Parasitol 61 (2015) 137–157.
[2] F. Di Pisa, G. Landi, L. Dello Iacono, C. Pozzi, C. Borsari, S. Ferrari, M. Santucci, N. Santarem, A. Cordeiro-da-Silva, C.B. Moraes, L.M. Alcantara, V. Fontana, L. H. Freitas-Junior, S. Gul, M. Kuzikov, B. Behrens, I. Pöhner, R.C. Wade, M.P. Costi, S. Mangani, Chroman-4-One derivatives targeting pteridine reductase 1 and showing anti-parasitic activity, Molecules 22 (2017) 426.
[3] P. Büscher, G. Cecchi, V. Jamonneau, G. Priotto, Human african trypanosomiasis, Lancet 390 (2017) 2397–2409.
[4] G. Landi, P. Linciano, C. Borsari, C.P. Bertolacini, C.B. Moraes, A. Cordeiro-da-Silva, S. Gul, G. Witt, M. Kuzikov, M.P. Costi, C. Pozzi, S. Mangani, Structural insights into the development of cycloguanil derivatives as trypanosoma brucei pteridine-reductase-1 inhibitors, ACS Infect. Dis. 5 (2019) 1105–1114.
[5] C. Borsari, A. Quotadamo, S. Ferrari, A. Venturelli, A. Cordeiro-da-Silva, N. Santarem, M.P. Costi, Chapter two - scaffolds and biological targets avenue to fight against drug resistance in leishmaniasis, in: M. Botta (Ed.), Annual Reports in Medicinal Chemistry, Academic Press, 2018, pp. 39–95.
[6] K. Stuart, R. Brun, S. Croft, A. Fairlamb, R.E. Gürtler, J. McKerrow, S. Reed, R. Tarleton, Kinetoplastids: related protozoan pathogens, different diseases, J. Clin. Investig. 118 (2008) 1301–1310.
[7] https://www.who.int/publications/i/item/9789240104440.
[8] W.M. de Souza, S.C. Weaver, Effects of climate change and human activities on vector-borne diseases, Nat. Rev. Microbiol. 22 (2024) 476–491.
[9] R. Capela, R. Moreira, F. Lopes, An overview of drug resistance in Protozoal diseases, Int. J. Mol. Sci. 20 (2019) 5748.

[10] J. Okombo, D.A. Fidock, Towards next-generation treatment options to combat Plasmodium falciparum malaria, Nat. Rev. Microbiol. 23 (2025) 178–191.
[11] S.P.S. Rao, U.H. Manjunatha, S. Mikolajczak, P.G. Ashigbie, T.T. Diagana, Drug discovery for parasitic diseases: powered by technology, enabled by pharmacology, informed by clinical science, Trends Parasitol. 39 (2023) 260–271.
[12] O. Valverde Mordt, A. Tarral, N. Strub-Wourgaft, Development and introduction of fexinidazole into the global human african trypanosomiasis program, Am. J. Trop. Med. Hyg. 106 (2022) 61–66.
[13] K.R. Tan, J. Hwang, Tafenoquine receives regulatory approval in USA for prophylaxis of malaria and radical cure of Plasmodium vivax, J. Trav. Med. 25 (2018), https://doi.org/10.1093/jtm/tay071.
[14] I.H. Gilbert, Drug discovery for neglected diseases: molecular target-based and phenotypic approaches, J. Med. Chem. 56 (2013) 7719–7726.
[15] C. Borsari, M.D. Jiménez-Antón, J. Eick, E. Bifeld, J.J. Torrado, A.I. Olías-Molero, M.J. Corral, N. Santarem, C. Baptista, L. Severi, S. Gul, M. Wolf, M. Kuzikov, B. Ellinger, J. Reinshagen, G. Witt, P. Linciano, A. Tait, L. Costantino, R. Luciani, P. Tejera Nevado, D. Zander-Dinse, C.H. Franco, S. Ferrari, C.B. Moraes, A. Cordeiro-da-Silva, G. Ponterini, J. Clos, J.M. Alunda, M.P. Costi, Discovery of a benzothiophene-flavonol halting miltefosine and antimonial drug resistance in Leishmania parasites through the application of medicinal chemistry, screening and genomics, Eur. J. Med. Chem. 183 (2019) 111676.
[16] C. Borsari, N. Santarem, S. Macedo, M.D. Jiménez-Antón, J.J. Torrado, A.I. Olías-Molero, M.J. Corral, A. Tait, S. Ferrari, L. Costantino, R. Luciani, G. Ponterini, S. Gul, M. Kuzikov, B. Ellinger, B. Behrens, J. Reinshagen, J.M. Alunda, A. Cordeiro-da-Silva, M.P. Costi, SAR studies and biological characterization of a chromen-4-one derivative as an anti-trypanosoma brucei agent, ACS Med. Chem. Lett. 10 (2019) 528–533.
[17] E. Uliassi, L. Piazzi, F. Belluti, A. Mazzanti, M. Kaiser, R. Brun, C.B. Moraes, L. H. Freitas-Junior, S. Gul, M. Kuzikov, B. Ellinger, C. Borsari, M.P. Costi, M. L. Bolognesi, Development of a focused library of triazole-linked privileged-structure-based conjugates leading to the discovery of novel phenotypic hits against Protozoan parasitic infections, ChemMedChem 13 (2018) 678–683.
[18] G.E. Magoulas, P. Afroudakis, K. Georgikopoulou, M. Roussaki, C. Borsari, T. Fotopoulou, N. Santarem, E. Barrias, P. Tejera Nevado, J. Hachenberg, E. Bifeld, B. Ellinger, M. Kuzikov, I. Fragiadaki, E. Scoulica, J. Clos, S. Gul, M.P. Costi, W. de Souza, K.C. Prousis, A. Cordeiro da Silva, T. Calogeropoulou, Design, synthesis and antiparasitic evaluation of click phospholipids, Molecules 26 (2021) 4204.
[19] F. Vincent, A. Nueda, J. Lee, M. Schenone, M. Prunotto, M. Mercola, Phenotypic drug discovery: recent successes, lessons learned and new directions, Nat. Rev. Drug Discov. 21 (2022) 899–914.
[20] V.K. Betu Kumeso, W.M. Kalonji, S. Rembry, O. Valverde Mordt, D. Ngolo Tete, A. Prêtre, S. Delhomme, M. Ilunga Wa Kyhi, M. Camara, J. Catusse, S. Schneitter, M. Nusbaumer, E. Mwamba Miaka, H. Mahenzi Mbembo, J. Makaya Mayawula, M. Layba Camara, F. Akwaso Massa, L. Kaninda Badibabi, A. Kasongo Bonama, P. Kavunga Lukula, S. Mutanda Kalonji, P. Mariero Philemon, R. Mokilifi Nganyonyi, H. Embana Mankiara, A. Asuka Akongo Nguba, V. Kobo Muanza, E. Mulenge Nasandhel, A. Fifi Nzeza Bambuwu, B. Scherrer, N. Strub-Wourgaft, A. Tarral, Efficacy and safety of acoziborole in patients with human African trypanosomiasis caused by Trypanosoma brucei gambiense: a multicentre, open-label, single-arm, phase 2/3 trial, Lancet Infect. Dis. 23 (2023) 463–470.
[21] E.K. Schmitt, G. Ndayisaba, A. Yeka, K.P. Asante, M.P. Grobusch, E. Karita, H. Mugerwa, S. Asiimwe, A. Oduro, B. Fofana, S. Doumbia, G. Su, K. Csermak Renner, V.K. Venishetty, S. Sayyed, J. Straimer, I. Demin, S. Barsainya, C. Boulton, P. Gandhi, Efficacy of cipargamin (KAE609) in a randomized, phase II dose-escalation study in adults in Sub-Saharan Africa with uncomplicated Plasmodium falciparum malaria, Clin. Infect. Dis. 74 (2022) 1831–1839.
[22] A.I. Corfu, N. Santarem, S. Luelmo, G. Mazza, A. Greco, A. Altomare, G. Ferrario, G. Nasta, O. Keminer, G. Aldini, L. Tamborini, N. Basilico, S. Parapini, S. Gul, A. Cordeiro-da-Silva, P. Conti, C. Borsari, Discovery of 1,3,4-oxadiazole derivatives as broad-spectrum antiparasitic agents, ACS Infect. Dis. 10 (2024) 2222–2238.
[23] A. Acharya, M. Yadav, M. Nagpure, S. Kumaresan, S.K. Guchhait, Molecular medicinal insights into scaffold hopping-based drug discovery success, Drug Discov. Today 29 (2024) 103845.
[24] A. Pinto, L. Tamborini, G. Cullia, P. Conti, C. De Micheli, Inspired by nature: the 3-Halo-4,5-dihydroisoxazole moiety as a novel molecular warhead for the design of covalent inhibitors, ChemMedChem 11 (2016) 10–14.
[25] A. Galbiati, S. Bova, R. Pacchiana, C. Borsari, M. Persico, A. Zana, S. Bruno, M. Donadelli, C. Fattorusso, P. Conti, Discovery of a spirocyclic 3-bromo-4,5-dihydroisoxazole covalent inhibitor of hGAPDH with antiproliferative activity against pancreatic cancer cells, Eur. J. Med. Chem. 254 (2023) 115286.
[26] T. Sahyoun, A. Arrault, R. Schneider, Amidoximes and oximes: synthesis, structure, and their key role as NO donors, Molecules 24 (2019) 2470.
[27] A.R. Gangloff, J. Litvak, E.J. Shelton, D. Sperandio, V.R. Wang, K.D. Rice, Synthesis of 3,5-disubstituted-1,2,4-oxadiazoles using tetrabutylammonium fluoride as a mild and efficient catalyst, Tetrahedron Lett. 42 (2001) 1441–1443.
[28] D.M. Vyas, Y. Chiang, T.W. Doyle, A short, efficient total synthesis of (±) acivicin and (±) bromo-acivicin, Tetrahedron Lett. 25 (1984) 487–490.
[29] T.T. Wager, X. Hou, P.R. Verhoest, A. Villalobos, Moving beyond rules: the development of a central nervous system multiparameter optimization (CNS MPO) approach to enable alignment of druglike properties, ACS Chem. Neurosci. 1 (2010) 435–449.
[30] J.I. Manzano, J. Konstantinović, D. Scaccabarozzi, A. Perea, A. Pavić, L. Cavicchini, N. Basilico, F. Gamarro, B.A. Šolaja, 4-Aminoquinoline-based compounds as antileishmanial agents that inhibit the energy metabolism of Leishmania, Eur. J. Med. Chem. 180 (2019) 28–40.
[31] M.A. Rason, T. Randriantsoa, H. Andrianantenaina, A. Ratsimbasoa, D. Menard, Performance and reliability of the SYBR Green I based assay for the routine monitoring of susceptibility of Plasmodium falciparum clinical isolates, Trans. R. Soc. Trop. Med. Hyg. 102 (2008) 346–351.
[32] M. Smilkstein, N. Sriwilaijaroen, J.X. Kelly, P. Wilairat, M. Riscoe, Simple and inexpensive fluorescence-based technique for high-throughput antimalarial drug screening, Antimicrob. Agents Chemother. 48 (2004) 1803–1806.
[33] M. Chugh, C. Scheurer, S. Sax, E. Bilsland, D.A. van Schalkwyk, K.J. Wicht, N. Hofmann, A. Sharma, S. Bashyam, S. Singh, S.G. Oliver, T.J. Egan, P. Malhotra, C.J. Sutherland, H.P. Beck, S. Wittlin, T. Spangenberg, X.C. Ding, Identification and deconvolution of cross-resistance signals from antimalarial compounds using multidrug-resistant Plasmodium falciparum strains, Antimicrob. Agents Chemother. 59 (2015) 1110–1118.
[34] S.H. Adjalley, G.L. Johnston, T. Li, R.T. Eastman, E.H. Ekland, A.G. Eappen, A. Richman, B.K. Sim, M.C. Lee, S.L. Hoffman, D.A. Fidock, Quantitative assessment of Plasmodium falciparum sexual development reveals potent transmission-blocking activity by methylene blue, Proc. Natl. Acad. Sci. U. S. A. 108 (2011) E1214–E1223.
[35] J. Reader, M.E. van der Watt, L.M. Birkholtz, Streamlined and robust stage-specific profiling of gametocytocidal compounds against Plasmodium falciparum, Front. Cell. Infect. Microbiol. 12 (2022) 926460.
[36] W. Trager, J.B. Jensen, Human malaria parasites in continuous culture, Science 193 (1976) 673–675.
[37] C. Borsari, R. Luciani, C. Pozzi, I. Poehner, S. Henrich, M. Trande, A. Cordeiro-da-Silva, N. Santarem, C. Baptista, A. Tait, F. Di Pisa, L. Dello Iacono, G. Landi, S. Gul, M. Wolf, M. Kuzikov, B. Ellinger, J. Reinshagen, G. Witt, P. Gribbon, M. Kohler, O. Keminer, B. Behrens, L. Costantino, P. Tejera Nevado, E. Bifeld, J. Eick, J. Clos, J. Torrado, M.D. Jiménez-Antón, M.J. Corral, J.M. Alunda, F. Pellati, R.C. Wade, S. Ferrari, S. Mangani, M.P. Costi, Profiling of flavonol derivatives for the development of antitrypanosomatidic drugs, J. Med. Chem. 59 (2016) 7598–7616.
[38] P. Baiocco, A. Ilari, P. Ceci, S. Orsini, M. Gramiccia, T. Di Muccio, G. Colotti, Inhibitory effect of silver nanoparticles on trypanothione reductase activity and Leishmania infantum proliferation, ACS Med. Chem. Lett. 2 (2011) 230–233.
[39] M.T. Makler, D.J. Hinrichs, Measurement of the lactate dehydrogenase activity of Plasmodium falciparum as an assessment of parasitemia, Am. J. Trop. Med. Hyg. 48 (1993) 205–210.
[40] C. Lambros, J.P. Vanderberg, Synchronization of Plasmodium falciparum erythrocytic stages in culture, J. Parasitol. 65 (1979) 418–420.
[41] L. Cevenini, G. Camarda, E. Michelini, G. Siciliano, M.M. Calabretta, R. Bona, T. R. Kumar, A. Cara, B.R. Branchini, D.A. Fidock, A. Roda, P. Alano, Multicolor bioluminescence boosts malaria research: quantitative dual-color assay and single-cell imaging in Plasmodium falciparum parasites, Anal. Chem. 86 (2014) 8814–8821.